



TAMPEREEN TEKNILLINEN YLIOPISTO  
TAMPERE UNIVERSITY OF TECHNOLOGY

INDRADUMNA BANERJEE

MEASUREMENT OF BEATING FORCE OF CARDIOMYOCYTES  
USING AN ATOMIC FORCE MICROSCOPE

Master of Science Thesis

Examiners: Professor Jukka Lekkala  
MSc. Tomi Ryyänen  
Examiners and topic approved by  
the Council of the Faculty of Engi-  
neering Sciences on April 9<sup>th</sup>, 2014.

## **Abstract**

TAMPERE UNIVERSITY OF TECHNOLOGY

BANERJEE INDRADUMNA:

Measurement of Beating Force of Cardiomyocytes Using an Atomic Force Microscope

Major subject: Mechatronics and Micromachines

Examiners: Professor Jukka Lekkala, MSc. Tomi Ryyänen.

**Keywords** – Cardiomyocytes, Beating force, Atomic force microscope.

**61 pages, 10 pages appendices**

The most commonly used transducer based methods for measurement of beating forces of cardiomyocytes have been reviewed in this thesis and they involve either direct contact with the cardiomyocytes or their manipulation in some way to measure the beating or contractile forces exerted by them. Other methods reviewed include advanced imaging techniques to capture the contraction and elongation of the cardiomyocytes from which the beating forces can be calculated. Atomic force microscope (AFM) was chosen as the most suitable measurement technique for quantifying beating forces of engineered cardiac tissues due to its long range of force measurement ranging from a few piconewtons to tens of micronewtons. Even though AFM has been used in the past to study cardiomyocytes but these efforts have required synchronizing the z piezo to the beating of the cardiomyocytes which created fluidic disturbances resulting in inaccurate measurements. This thesis work demonstrates a novel method using the AFM to measure the beating forces of cardiomyocytes. In this method, the AFM tip is kept stationary and lowered on top of the sample and the z piezo is locked in its position. Now, the tip gently touches the sample surface with a minimal contact force. The stationary tip on coming in contact with the beating cardiomyocyte sample experienced deflections in the up and down directions which on multiplying with the spring constant of the probe gave the value of beating force. AFM was also used to quantify the mechanobiological properties of pluripotent, stem cell-derived cardiomyocytes, including frequency of beats, duration, and cellular elasticity. The elasticity of some known standard samples like PDMS was measured in order to ascertain the long range of measurements as well as the accuracy of the AFM. The beating forces were observed both over a single cardiomyocyte as well as over a cluster of beating cardiomyocytes and it was found that for clusters, the beating forces exerted were higher and more rhythmic. The AFM-based method described in this thesis can serve as a screening tool for the development of cardiac-active pharmacological agents, or as a platform for studying cardiomyocyte biology.

## PREFACE

I would like to take this opportunity to thank all the persons who have contributed towards making this thesis successful. The thesis was completed at the department of Automation Science and Engineering and I am thankful to all the staff members in the department for maintaining an excellent working environment. I would like to especially thank my tutor, Prof. Jukka Lekkala for his support, continuous supervision and quality inputs. Working on this thesis has been a significant challenge for me and without his help I am convinced I could not complete this thesis successfully. Most importantly, I also want to thank him for giving me this wonderful opportunity to work in a TEKES funded Human spare parts project.

Same goes to my supervisor Tomi Ryyänen whose inputs helped me to draft my work in the form of a thesis. I must equally thank my trainer Maiju Hiltunen for spending quality time in training me with the atomic force microscope (AFM). She also provided me with very helpful literature during the course of my thesis which really helped me understand what I needed to do.

I am also grateful to Marisa Ojala and Henna Venäläinen from the Heart Group for training me with the END 2 and cardiomyocyte samples under the optical microscope, for providing me with enough number of samples for validating my results and also providing various literature which helped during the course of the thesis. I also need to thank Janne Koivisto for sharing his experiences with the AFM.

I am also thankful to Prof. Minna Kellomaki for arranging for expert training with the device. The same goes to Prof. Katriina Aalto-Setälä for presenting a really challenging topic for my thesis.

I also need to mention the role of Joose Kreutzer and Marlitt Viehrig from the Microsystem Technology Group. They provided with the PDMS samples which were used as reference samples during elasticity measurements.

My heart felt appreciation to the staff at BioMediTech and the Analysing Laboratory in the Electronics and Communication Department for providing a conducive environment to work.

I am thankful to my girlfriend for being with me when I was going through this terribly busy time writing my thesis. Finally, I want to thank God for being with me during all stages of my life including this one.

Tampere, August 12, 2014

Indradumna Banerjee  
Finninmäenkatu 4L105  
33710 Tampere

## TABLE OF CONTENTS

Abstract.....	0
Preface.....	1
Abbreviations and Notations.....	3
1. Introduction .....	5
2. Methods for force measurement.....	8
2.1 Transducer based methods for force measurement.....	8
2.2 Image based methods .....	17
2.3 Summary of the methods of force measurement .....	21
3. Atomic Force Microscope: The most suitable method .....	24
3.1 Atomic Force Microscope: Basic concepts .....	24
3.2 XE100 SPM Stage.....	25
3.3 Modes of operation.....	26
3.4 Liquid cell imaging .....	28
3.5 Cantilever selection procedure.....	26
3.6 Force distance spectroscopy .....	29
3.7 AFM XE 100 Software.....	31
4. Methods and Materials.....	35
4.1 Sample preparation method: Beating cardiomyocyte and fixed non beating cardiomyocyte .....	35
4.2 Sample preparation method: PDMS Structures .....	37
4.3 AFM probing of elasticity and interaction forces .....	38
5. Results and Discussion.....	40
5.1 PDMS samples imaging and Young's Modulus Calculation.....	40
5.2 End 2 cells and cardiomyocytes: Imaging and Young's Modulus Measurements.....	43
5.3 Beating force of cardiomyocytes .....	48
6. Conclusion.....	54
References .....	57
APPENDIX.....	62

## ABBREVIATIONS AND NOTATION

AFM	Atomic force microscope
iPSC	Induced pluripotent stem cells
END2	Visceral endothelial like stem cells
CCD	Charge coupled device
PSPD	Position sensitive photo detector
CF	Carbon fiber
PZT	Piezoelectric tube
K	Stiffness constant of carbon fiber
$\Delta L_f$	Change in carbon fiber tip position from initial position
$\Delta L_p$	Change in piezoelectric tube tip position from initial position
CMT	Cardiac microtissues
MEMS	Micro electromechanical systems
ECM	Extra Cellular matrix
PDMS	Polydimethylsiloxane
SPM	Scanning Probe Microscope
NC-AFM	Non-contact mode operation of AFM.
C-AFM	Contact mode operation of AFM
Q-Factor	Quality Factor
F-d Spec.	Force distance Spectroscopy mode of AFM
XEC	Camera Software of Park Systems AFM XE-100
XEP	Data Acquisition Software of Park Systems AFM XE-100
XEI	Image Processing Software of Park Systems AFM XE-100
DMEM	A basal medium optimized for growth of undifferentiated embryonic and pluripotent stem cells.
MEF	Murine Embryonic Fibroblasts feeder cells.
KSR	Knockout Serum Replacement Medium
PBS	Phosphate Buffered Saline
ACTA	AFM Cantilever designed for Non-Contact / Tapping Mode / Intermittent Contact / Close Contact applications.
SU-8	Permanent epoxy negative photoresist
O <sub>2</sub>	Oxygen
W	Watt
Hz	Hertz
kHz	Kilohertz
E	Young's modulus of elasticity
F(h)	Force of interaction between cardiomyocyte sample and tip of AFM cantilever.
H	Distance of approach of the cantilever to the sample surface.
$\nu$	Poisson's ratio
nN	Nanonewtons
MPa	Megapascals

R            Radius of tip of AFM cantilever  
sqcm        Square centimeters

..

# 1. INTRODUCTION

Induced pluripotent stem cells (iPS) discovered as recently as in 2006 for mouse cells [1] and in 2007 for human beings [2] are cells with the ability to differentiate into any of the three germ layers: endoderm (interior stomach lining, gastrointestinal tract, the lungs), mesoderm (muscle, bone, blood, urogenital), or ectoderm (epidermal tissues and nervous system) [3]. Due to this property, there is an increasing amount of research on the possibility of using the iPS cells to generate spare organs or parts for damaged critical organs in the human body [4], one of the most important being the human heart. As these cells originate from the human body itself, there are less chances of immune rejection by the body and they also come with a huge potential of supplying large quantities of patient-specific cells for cardiac repair. Generation of human spare parts is still a distant future concept but patient specific iPS cell derived cardiomyocytes are being used extensively for disease modelling of genetic heart diseases, studying the effect of some cardiac drugs on the beating force of cardiomyocytes [5], as well as for screening of drugs related to cardiac diseases [6]. Use of iPS cell derived cardiomyocytes will require careful characterization of their properties. If it is possible to measure contractile properties of a single cardiomyocyte, then it can lay the foundation for quantitatively understanding the mechanism of heart failure and molecular alterations in diseased heart cells. One of the contractile properties is the beating force of cardiomyocytes which is the force of contraction and expansion when a cardiac muscle pumps blood and maintains blood pressure.

The thesis starts with a review of the existing methods for force measurement of beating heart cells in a systematic manner and also presents the limitations and advantages that are associated with the implementation of each of these methods. After the methods have been described in sufficient detail, a logical reasoning follows on why atomic force microscopy (AFM) was chosen as the most appropriate method for force measurement of beating cardiomyocytes.

The existing methods for the force measurement can be classified into two categories, transducer based methods and image based methods. The transducer based methods for force measurement use tools that generate some forces or mechanically deform the cells in some way. AFM, which is an example of the transducer based methods, uses a sharp tip to probe the cell sample and the deformation of the tip with respect to the cell sample can be used to determine the force generated by the cell [7-10]. Even though this method has been used several times but the scan area of an AFM is lesser than the area occupied by one single cardiomyocyte. Another transducer based method is use of magnetic beads which involve attaching a magnetic bead to the cell and applying a magnetic field to move it linearly or twist it [11]. But then there are some problems associated with this method too like beads losing magnetization over time as well as challenges in controlling the properties of the bond or linkage between the magnetic beads and cell. Other transducer based methods include using elastimetry or cell drum [12-

19], carbon fiber based systems [20, 21], or force sensors [22-27]. Each of these methods will be discussed in detail in the second chapter. The optical or image based methods of force measurement are different from the transducer based methods in the sense that they involve measuring deflections from reflective or transparent substrates on which the cells are cultured, through light microscopy and then calculating the force through some complex mathematical formulations like deconvolution. One technique is culturing cardiomyocyte cells on flexible sheets with some pattern [28-30], either a grid or dot or beads [31] but these methods involve using complex deconvolution to measure force from the displacements. All the commonly used optical methods [32-40] and the limitations and advantages associated with each of them have been discussed in good details in this review. The force measured by these methods typically range from the piconewton to nanonewton range except the AFM which can measure from a few piconewtons to a few tens of micronewtons or more. After a review of the existing methods, their suitability for measuring the beating force of a single heart cell is also discussed in the second chapter of the thesis.

AFM was chosen as the most suitable method for beating force measurements of single heart cells or a cluster of cells. However, what is reported as “beating force” of heart cells in the reviewed works, as well as throughout this thesis is actually a measured signal of the displacement of the AFM cantilever tip as the cardiomyocytes interact with it. The displacement of the AFM cantilever is only in the vertical direction, so it does not take into account the lateral contraction and expansion of the cardiomyocytes. The displacement of cantilever is multiplied with the spring constant of the cantilever which gives a force which is definitely proportional and very close to the actual beating force of the cardiomyocyte but might not be exactly equal to it. This is true for the beating forces reported by most of the other methods as well.

There were several reasons behind choosing AFM as the most suitable method. Firstly, wide range of forces from piconewtons to micronewtons range can be measured with the atomic force microscope (AFM) and the AFM is calibrated at all these values by the manufacturer of the device itself. The accuracy of a commercially available device is more trustworthy compared to a device made by a particular research group or person. Also as AFM is a commercially available device, there are no initial setup hassles of the system for beating force measurements and this gives AFM a distinct advantage over other methods. But then mastering the use of AFM normally takes a long time as well as lots of training.

A novel approach for measuring the beating forces of cardiomyocytes has been presented in this thesis, in which the AFM was directly lowered on top of the beating cells at a very low contact force and then the nanoscale tip of the AFM was kept stationary. Normally, under such circumstances in a static medium nothing should be recorded but in a dynamic medium with the beating cells a constant up and down displacement of the cantilever was recorded. The displacement multiplied by the spring constant of the cantilever gave the forces which a cardiomyocyte was able to generate against the probing tip of the cantilever and this should be proportional and very close to the beating forces

of the cardiomyocyte, for reasons described earlier. The success of this approach meant that for the first time, the beating forces of stem cell derived cardiomyocytes were reported with an AFM without synchronization of the z axis piezo actuator to the beating of the cardiomyocytes. AFM has been used to study cardiomyocytes in the past [7, 9] but these efforts required synchronizing the z-piezo of the AFM with beating of the cardiomyocytes, which created fluidic disturbances that prevented accurate measurement of contraction forces. Our method is to touch the cell gently with the AFM cantilever, then lock the z-piezo, which forces contractions of the cell to deflect the cantilever.

The third chapter of the thesis is devoted to understanding the basics as well as the most important concepts related to AFM. The fourth chapter describes the sample preparation methods for cardiomyocyte and mouse visceral endothelial like cells (END-2). It also gives detailed description of the theory behind the calculation of cell elasticity and beating forces of cardiomyocytes. The fifth chapter presents an analysis of the results obtained during the course of the thesis. It includes the images taken by the AFM, the force distance spectroscopy graphs, the calculated elasticity for both cardiomyocytes and END 2 cells and finally the beating forces of cardiomyocytes. Finally, the thesis concludes by summarizing the most important achievements in the thesis as well as the future directions where the results of this thesis can be used.

## 2. METHODS FOR FORCE MEASUREMENT

This chapter presents a literature review on the existing methods for force measurement in cardiomyocytes. As already discussed, they have been grouped into two major categories, transducer based measurement methods and optical measurement methods.

### 2.1 Transducer based methods for force measurement

The transducer based methods for force measurement involve measuring cell deformation using tools that generate tensile, shear, bending or twisting forces. Most of the transducer based methods and the advantages and limitations associated with measuring the beating force of heart cells using them has been discussed in details in this section.

#### a. Atomic Force Microscopy

Atomic Force Microscope (AFM) has emerged as a powerful tool in studying cellular interactions in cardiovascular research. It has a probe comprising a cantilever (dimensions on the order of micrometers) with a nanoscale tip (dimensions on the order of nanometers). The AFM is capable of manipulation in the x, y and z directions, capable of providing high sensitivity up to piconewtons, spatial resolution up to nanometers, 3D surface topographical imaging and directly measuring mechanical properties in *invitro* isolated cells.

The beating force of a cardiomyocyte can be determined by interactions with a nanoscale tip of an AFM cantilever, with or without functionalization of the nanoscale tip. Functionalization of the nanoscale tip can be defined as attaching by covalent or non-covalent means, a ligand or receptor to the tip and a counter ligand or receptor should be there on the surface of the cardiomyocyte. The ligand and receptors in cardiomyocytes are normally known to the biologists and can be obtained from specialized pharmaceutical companies. While functionalization is one of the latest inventions in this field [10], the measurements can be done with an AFM tip even without functionalization [7]. The tip of the AFM cantilever makes contact on the surface of the cardiomyocyte, and as the cardiomyocyte starts beating, it induces vertical fluctuations in the signals recorded. From these vertical fluctuations, the force of the beating cardiomyocytes can be recorded.

An experimental setup using an AFM is shown in Figure 2.1, in which the nanoscale tip is rigidly attached to a micromachined cantilever beam. Depending on the distance between the atoms at the tip of the cantilever and those at the sample's surface, there

exists either an attractive or repulsive interaction force that may be utilized to measure the sample surface. The tip of the cantilever deflects due to force between the atoms at the sample's surface and those at the cantilever's tip. The laser beam which is focused on top of the cantilever is used to quantify the cantilever deflection and a Position Sensitive Photo Detector (PSPD) detects the laser beam. The tube-shaped piezo scanner is responsible for horizontal direction (X-Y) and vertical direction (Z) movement of the sample. The tube shaped scanner scans the sample line by line continuously, while a feedback loop controlled by the PSPD signal controls the vertical movement of the scanner as the cantilever moves across the sample surface [8].

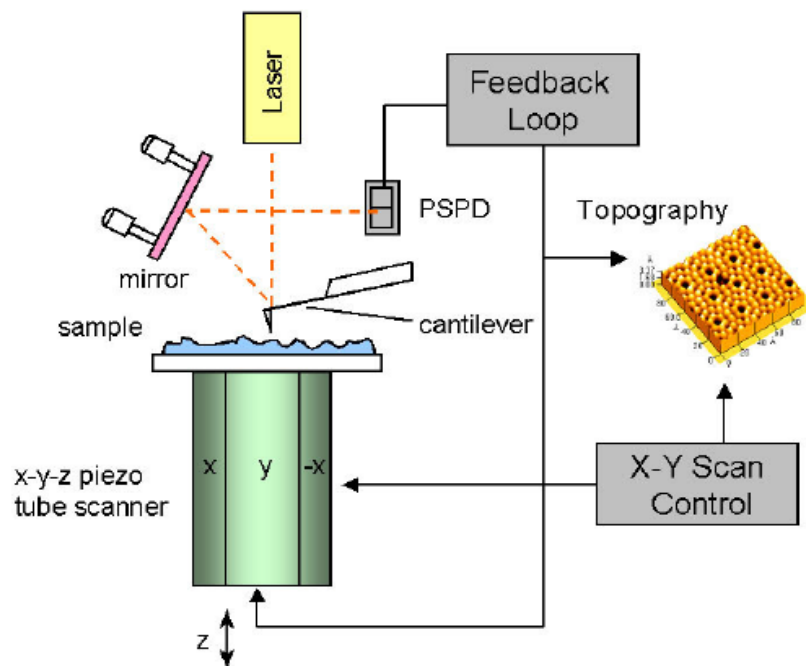


**Fig 2.1. Schematic representation of an atomic force microscope [8].**

The whole setup is thus acting as a feedback loop. The cantilever goes from its starting position to the position when it makes contact with the cell. After imaging or tip sample interaction force measurements, the probe retracts until the bond between the probe and the cell ruptures and finally it goes back to its starting position. The range of forces measured can be up to the order of piconewtons [8]. AFM has also been used to investigate the viscous and elastic properties of endothelial, cardiac and skeletal muscle cells [9].

This method however has a few limitations. One of the most important is the single scan image size. The maximum imaging height of AFM can be of the order of 10 to 20 micrometers and maximum scanning area of 150 by 150 micrometers. This is much less in comparison to a Scanning Electron Microscope (SEM) whose imaging area is of the order of square millimeters with a depth of field or imaging height of the order of millimeters. For measuring the beating forces of cardiomyocytes during the course of this thesis, Park systems AFM XE 100 was used, which had a maximum

scanning area of only 45 micrometers by 45 micrometers, not enough to image an entire cardiomyocyte. Also, it takes some time to practise with the AFM, possibly months of imaging before someone can get the parameters right to image in liquid.

### b. Cell drum, elastimetry and use of stretching devices

The principle of the elastimetry technique is applying a gentle suction force on the surface of the cardiomyocyte through a micropipette like structure. This suction force results in a small deflection produced on the cardiomyocyte. The geometry of the resulting deformation together with the applied pressure can be used to derive the mechanical properties of the cell [12-14]. The principle is illustrated in figure 2.2 below.

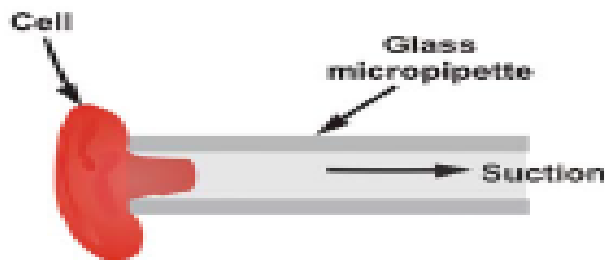


**Fig.2.2. Schematic explaining the principle of elastimetry of representative human red blood cell [10].**

The deformation produced in the cell shown above could be captured by advanced imaging methods. The elastimetry technique based methods, however, lacked easy-to-use handling procedures.

Cell drum is an improvement on the existing methods of elastimetry and use of stretching devices. It can be used to measure the pressure of contraction and expansion in cardiomyocytes and if the pressure can be measured, the force can be also measured as the dimensions of the cell drum are known. This method has been successfully used to measure the contractile tension and beating rates of self-exciting monolayers and 3D tissue constructs in neonatal rat cardiomyocytes [15-17]. The cylindrical cell drum (diameter 16 mm, height 8 mm) as shown in Figure 2.3 has a thin and flexible silicone membrane covering. It is fitted into a chamber having a pressure sensor (Validyne CD 223) and a laser-based deflection sensor (Keyence LK-G 32) [15].

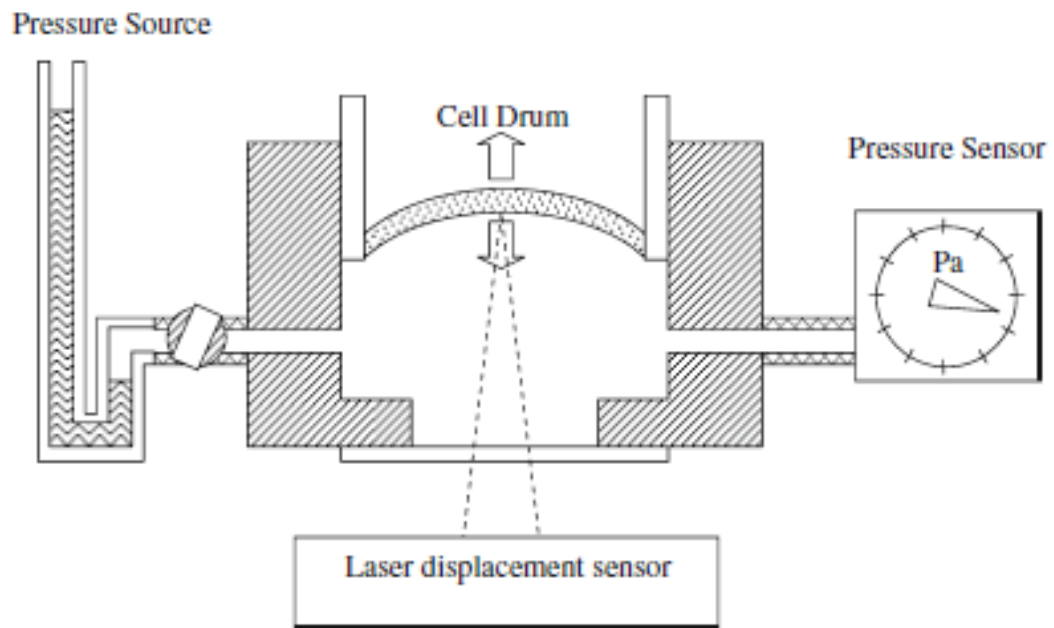


**Fig. 2.3. Experimental Setup for measuring contraction rate and mechanical tension of self-exciting cardiomyocytes with an air-tight chamber covered with the cell drum and the cell layer on top of it [15].**

A small pump in the pressure source bulbs the membrane upwards by about 1.5 mm. The drum material is a thin layer of silicone sheet of about a few micrometer thickness. Some kind of surface treatment with laminin is necessary so that the cells stick to the surface of the cell drum. The cell culture medium containing the beating cardiomyocytes is placed above the cell drum with utmost care. Now, when the cardiomyocytes start beating, there are two kinds of pressure acting on the cell drum, one is the residual offset pressure because of the cell culture medium and the small pump and the second is the pressure due to beating of the cardiomyocytes. The laser deflection sensor records the membrane deflection when the cardiomyocyte starts beating. This allows the calculation of the change in chamber volume and strain. As the residual pressure is recorded earlier, the new deflection and pressure due to beating of the cardiomyocytes is recorded. The difference of the original residual pressure and the new pressure recorded is the differential pressure which is exerted by the beating of the cardiomyocyte. From the differential pressure recorded, the beating force can be calculated as the strain produced is known from the deflection sensor, as well as dimensions of the cell drum is known. A typical force time curve of a beating cardiomyocyte obtained with the cell drum method is shown in Figure 2.4. The high noise seen in the figure can be filtered with a low pass Butterworth filter and a rhythmic pattern can be seen in it which proves that the beating of the cardiomyocyte cells has been recorded [15].

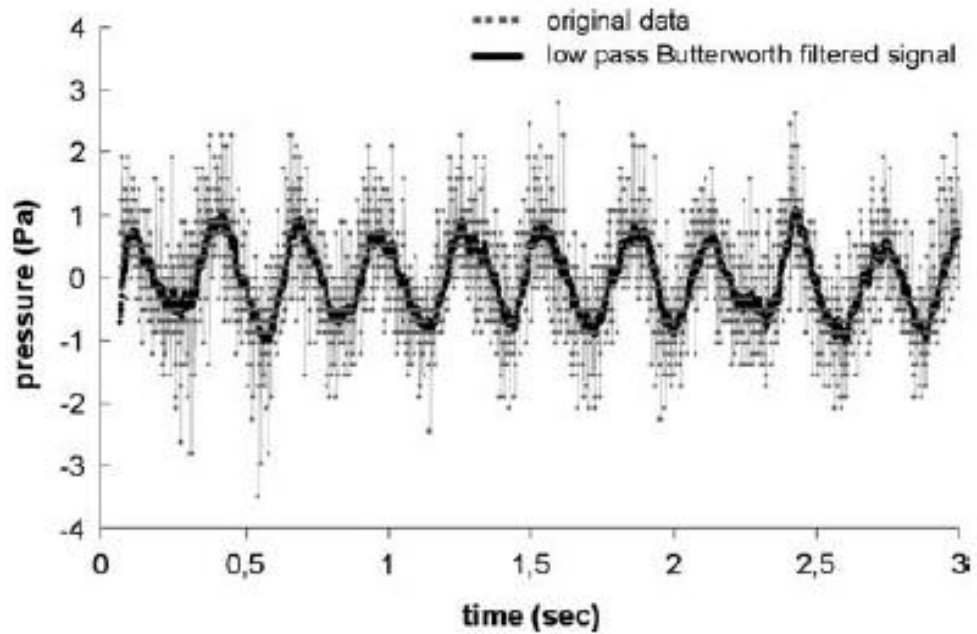


**Fig. 2.4. Contractile pressure of cardiomyocyte measured as a function of time from a 3D tissue construct of beating cardiomyocytes [15].**

The force measurement possible with this method is typically around 0 to 100 nanonewtons and even though this method is an improvement on the previously existing methods of elastimetry and cell stretching devices it still has some limitations. Firstly, it requires extreme carefulness to isolate a single beating cardiomyocyte in this method. Also, the signals obtained require a lot of filtering for the correct rhythmic patterns to be observed reducing the accuracy of the method.

### **c. Attaching magnetic beads**

Another method to measure beating forces of cardiomyocytes is by attaching magnetic beads. Small magnetic particles called magnetic beads can be attached to the cardiomyocytes through some special arrangements. The operation using these magnetic beads requires presence of an external magnetic field, and when the cardiomyocyte contracts, the contractile force can be recorded by the change in magnetic field. Initially, a field-stimulated contraction of single cardiomyocyte as a function of time and applying magnetic field is recorded. This simulation is carried out without attaching the magnetic bead. This is followed by applying a magnetic field on the attached magnetic bead and recording the reduction in contraction. For attaching the magnetic bead to a single cardiomyocyte, a preliminary coating with some cellular adhesive substance like laminin or extra cellular matrix is done. The contraction of the cardiomyocytes is observed by an inverted microscope with a high resolution CCD video camera. On application of the magnetic field, there is supposed to be a reduction in contraction which can be captured by the CCD video camera. When the fractional shortening of cardiomyocyte in the pres-

ence and absence of magnetic field is plotted together in the same graph, the estimated internal contraction force of the cardiomyocyte can be calculated as a function of the initial contraction, final contraction and the external magnetic force applied. The forces generated by the cardiomyocytes, of the order of a few nanonewtons can be successfully measured with this method. This principle is aptly described in figure 2.5. The beads are made of nickel having a radius of about 10 micrometers and the external magnetic field force varies from a few piconewtons to a few micronewtons as the magnetic field (function of distance between magnetic bead and solenoid) is varied. The magnetic field is generated by a thin coil solenoid with the following parameters: number of turns:  $N = 5000$ , diameter of solenoid:  $D = 5$  mm, length of solenoid:  $L = 50$  mm, and the current passing through solenoid:  $I = 0.5$  A. The maximum magnetic field intensity applied is  $1 \times 10^7$  A/m [11].

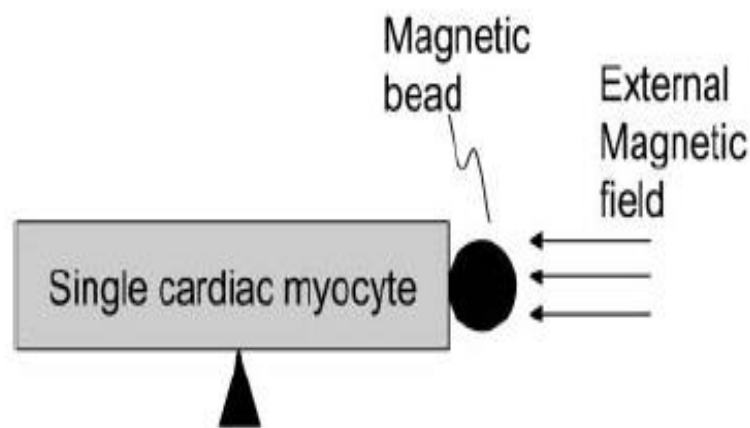


**Fig 2.5. External magnetic field acting on a single cardiomyocyte with magnetic bead attached [11].**

There are however some difficulties associated with this method like controlling the region of the cell to which the beads bind. Depending on the attachment at the periphery or near the nucleus of the cell, measurements of the mechanical properties will be different. Next, if the beads do not completely bind to the cell surface, then it can result in underestimation of cell stiffness. Also, the beads lose magnetization with time and must be re-magnetized at specific time intervals to maintain the torque applied. Also, one issue is that it is not established whether the cells behave normally when the beads are attached even though the forces reported are within the expected range. Another issue is that the beads probably cannot be removed after the beating force measurements, so the cells become useless after the force measurements.

#### d. Carbon fiber based systems

Carbon fiber (CF) is a material consisting of fiber about 5–10 micrometer in diameter and composed mostly of carbon atoms. The carbon atoms are bonded together in crystals that are more or less aligned parallel to the long axis of the fiber. In this method, a pair of carbon fibers is attached to each end of the cardiomyocyte through micro manipulators. Bidirectional position control along one axis (say x axis) is achieved with a pair of high accuracy piezoelectric tubes (PZT). The myocyte and CF tips are monitored through an inverted microscope. The length of the cardiomyocyte and the CF tips are recorded at high frequency imaging in real time [20,21]. Active and passive forces ( $F$ ) are calculated from CF bending, assessed by monitoring CF tip and PZT positions as expressed by equation 2.1.

$$F = K (\Delta L_f - \Delta L_p) \quad (2.1)$$

Here,  $\Delta L_p$  and  $\Delta L_f$  are the change in the original distances between the PZT tube holders and the CF tips respectively.  $K$  is the stiffness constant of the CF and can be measured using a force transducer system. The force detection limit of the sensor was found to be 5 micronewtons as the upper limit and the lower limits around a few nanonewtons [20,21]. A schematic diagram of the carbon fiber based system is shown in Fig. 2.6.

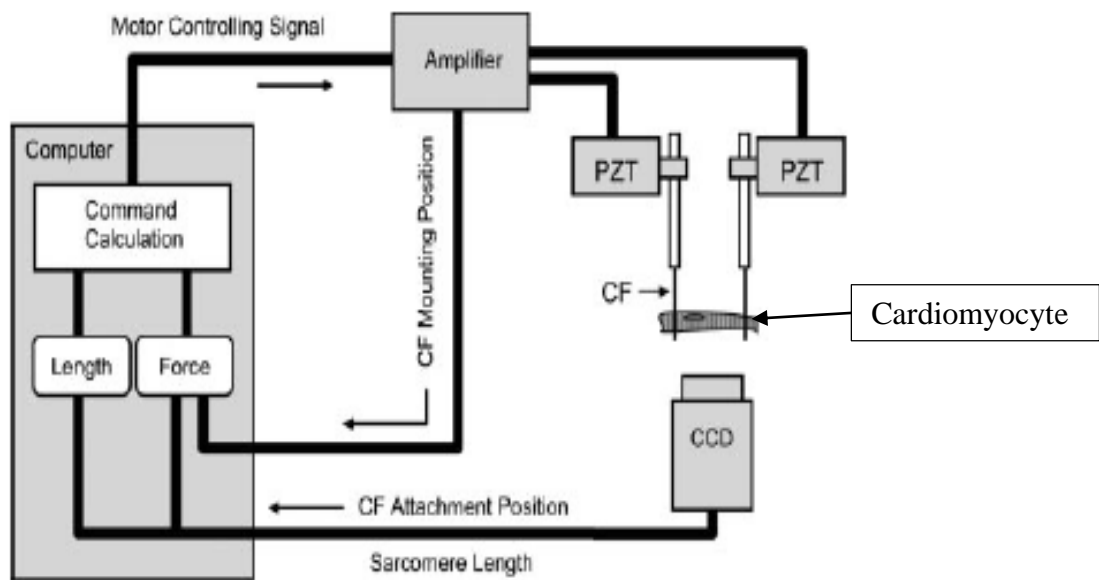


**Fig 2.6. Schematic diagram of force measurement in cardiomyocyte using carbon fibers [18].**

In spite of the success of carbon fiber-based analysis, some concerns were reported as to some kind of damage of the cardiomyocyte's ends, the various difficulties associated in

obtaining uniform sarcomere spacing, and also the fact that the system allows full activation of the cells only at short sarcomere lengths [19]. Sugiura's method [20] addresses the first concern of attaching single cardiomyocytes to carbon fibers for mechanical manipulation and measurement by using cell-adhesive carbon fibers that attach easily to the cell membrane without causing noticeable damage.

#### e. Micro force sensors and force transducers

Another commonly used method as well as one of the methods mostly used recently to measure beating forces in cardiomyocytes involve using advanced force sensors and transducers. Some researchers have used commercially available microforce sensors like FRS-711, Koyo precision [22, 23]. The microforce sensor has a probe which on coming in contact with the beating cell provides an output voltage proportional to the force [41]. One example of micromachined force sensors is shown in Fig 2.7 in which a single cell is placed on a cell platform (CP). Displacement was applied on one half of the platform (PA) and the other half was mechanically linked to a sensor which can measure the force on a cell. The actuation was provided by an off-chip, computer controlled piezoelectric stage while the sensor was several cantilever beams in parallel [42].

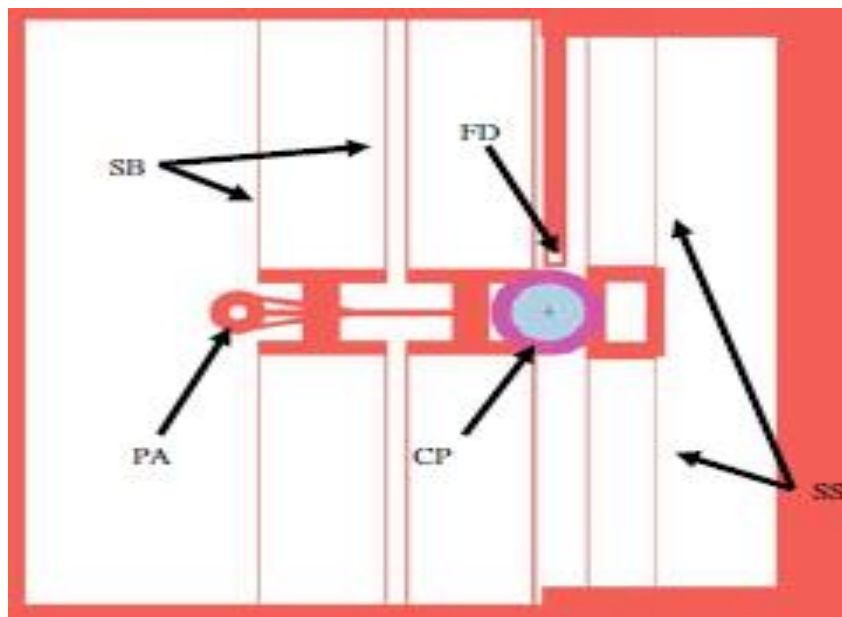


**Fig. 2.7. Schematic drawing of a uniaxial BIOMEMS device for quantitative force measurements of a single cell. CP is the cell platform, SB is the support beams for the annulus PA and the sensor springs SS [42].**

The exact relation between the output voltage and the measured force is not known and hence the sensor needs to be calibrated relative to a known reference to achieve accurate measurements. A custom-built calibration system is used for the calibration of each individual sensor. A force applied to the probe in axial direction leads to relative motion of the body and the outer frame, which is measured by two electrode arrays as a change in electrical capacitance and converted to an analog voltage using a capacitance to volt-

age converting integrated circuit. Microcantilever based force sensors have also been successfully used to measure beating forces of heart cells [24, 25]. Cantilever spring constants are first calculated using a capacitive MEMS force sensor mounted on a micromanipulator. In the cell culture medium where cardiac microtissues (CMT) are developed, a large array of CMTs or a single CMT are anchored to the tips of the cantilevers per substrate. Linear bending theory and experimental measurements is used for reporting the spring constant for with some samples of PDMS and curing agent whose stiffness values are known. These spring constants obtained were then used to link the measured cantilever deflections to the amount of force generated by CMTs. Force transducers like FT-03C, Grass Instrument Company [26] and BAM7C, Scientific Instruments [27] have also been successfully used to measure the beating forces of human heart cells.

## 2.2 Image based methods

Three of the most commonly used image based methods of force measurement are described in this section. These methods involve advanced imaging techniques and no physical contact with the cells.

### a. Flexible sheets with various patterns

A number of efforts to measure the contractile force exerted by tissue cells have been made with flexible substrates with micropatterned grids or dots or embedded beads. It was first proposed by Harris in 1980 [28] that when tissue cells are cultured on very thin sheets of cross linked silicone fluid, the forces the cells exert are made visible as elastic distortion and wrinkling of the substratum as shown in Fig.2.8. The cells were treated with extra cellular matrix (ECM) proteins for better cell adhesion and attachment [28].

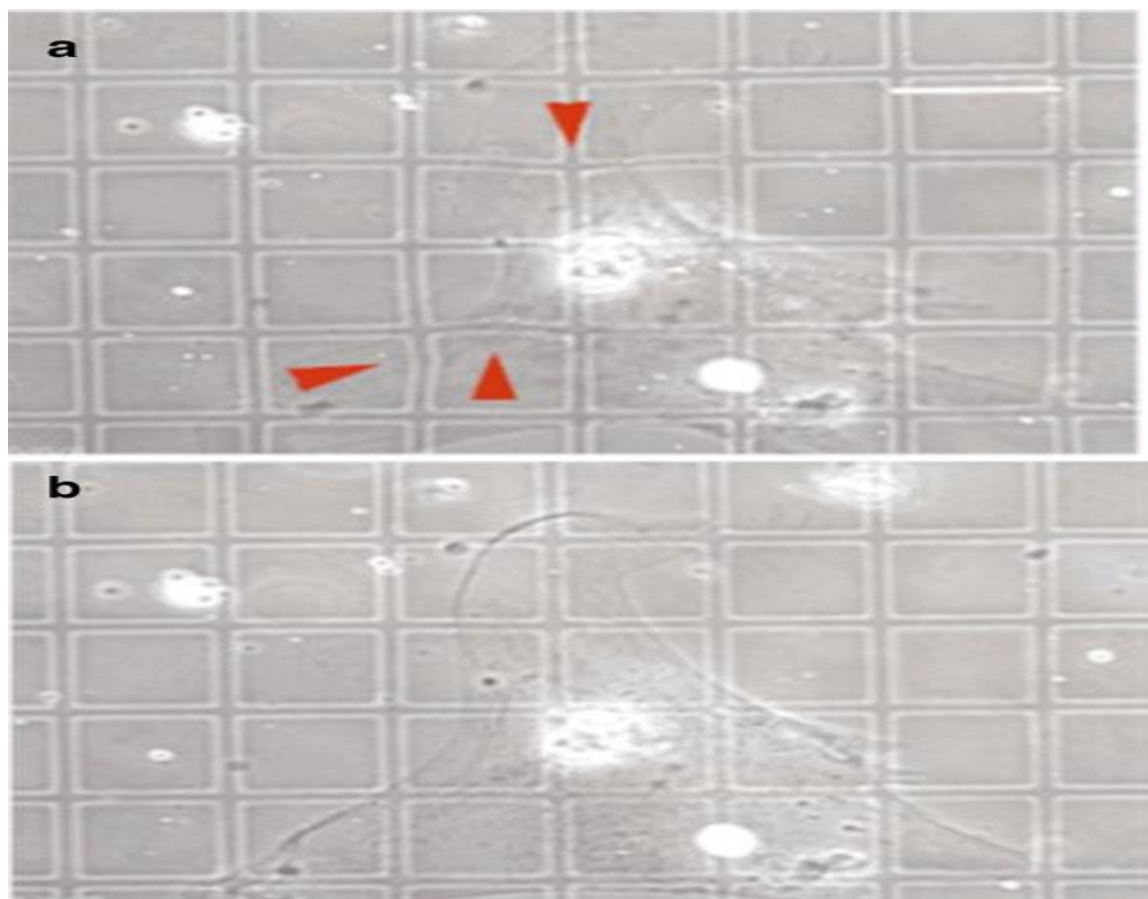


**Fig 2.8. Small thin silicone sheets with deformation patterns (shown by red arrows) developed during the contraction and expansion cycle of rat fibroblast(a) and cardiomyocytes(b) on a large grid [30]**

However, the distortions were observed to be extremely chaotic in shape as well as non linear. The deformation data could only be quantitatively analyzed with this technique as the buckling of thin polymer films is a nonlinear phenomenon that is very difficult to treat in elasticity theory. Lee and his group [29] modified this method with fluorescent latex beads. The idea behind this was suppressing the wrinkling of the film by prestressing it thus allowing only tangential deformation which can be tracked with the fluorescent latex beads. The main flaw in this approach was however that the measured displacements were assumed to be in respect to a single bead displacement only. It was necessary that the displacements due to the other beads in the sheet also needed to be taken into account and added to get the correct total displacement of a single bead. This was addressed by Dembo and Wang [31] using statistical methods. Balaban's group [10] used sheets with micropatterned dots and grids to measure the traction forces exerted by rat cardiomyocytes and endothelial cells and were able to compute the forces generated at the focal adhesions using elastic theory based on the semi-infinite space. They assumed that the forces originate from the measured locations and do not propagate across the substrate. They solved the inverse problem of computing the tractions given the displacements using least square minimization techniques. Using this method they reported maximum traction forces of 20 nN for rat cardiac fibroblast cells and 70 nN for rat cardiac myocytes [10].

## **b. Optical monitoring**

Optical monitoring involves frame by frame capture of the activities of cardiomyocytes through a high resolution confocal microscope [31-35]. In this technique, microposts are calibrated using a piezoresistive microcantilever [32,33]. Force is calculated from voltage out of the Wheatstone bridge and displacement is measured optically using an upright microscope.

Once these microposts are created, then a piezoresistive cantilever is made to touch the surface of these microposts and the displacement of these cantilevers are measured by an upright microscope optically. Then the signal is actually coupled to a Wheatstone bridge and the change in resistance tells the force generated with proper calibration. Forces as small as a few nanonewtons can be measured with this method.

Laurie et al. [34] developed a force measurement technique of contractile heart tissues which depends on frame by frame capture of the contraction of heart cells from its resting state and then using theoretical calculations to determine the force generated during contraction. The basis for these theoretical calculations was the same as proposed by Dembo and Wang [31]. Cells were maintained at 37°C during imaging by placing them on a heated ring connected to a temperature controller. Contracting cells were imaged using a confocal microscope with a 20x objective. To quantify contraction stress, one frame corresponding to the maximum point of the contraction cycle, where the cell was at its point of maximum contraction and one frame corresponding to the minimum point

of the contraction cycle, where the cell was at rest were identified for each contracting cell. This is shown nicely in Fig.2.9.

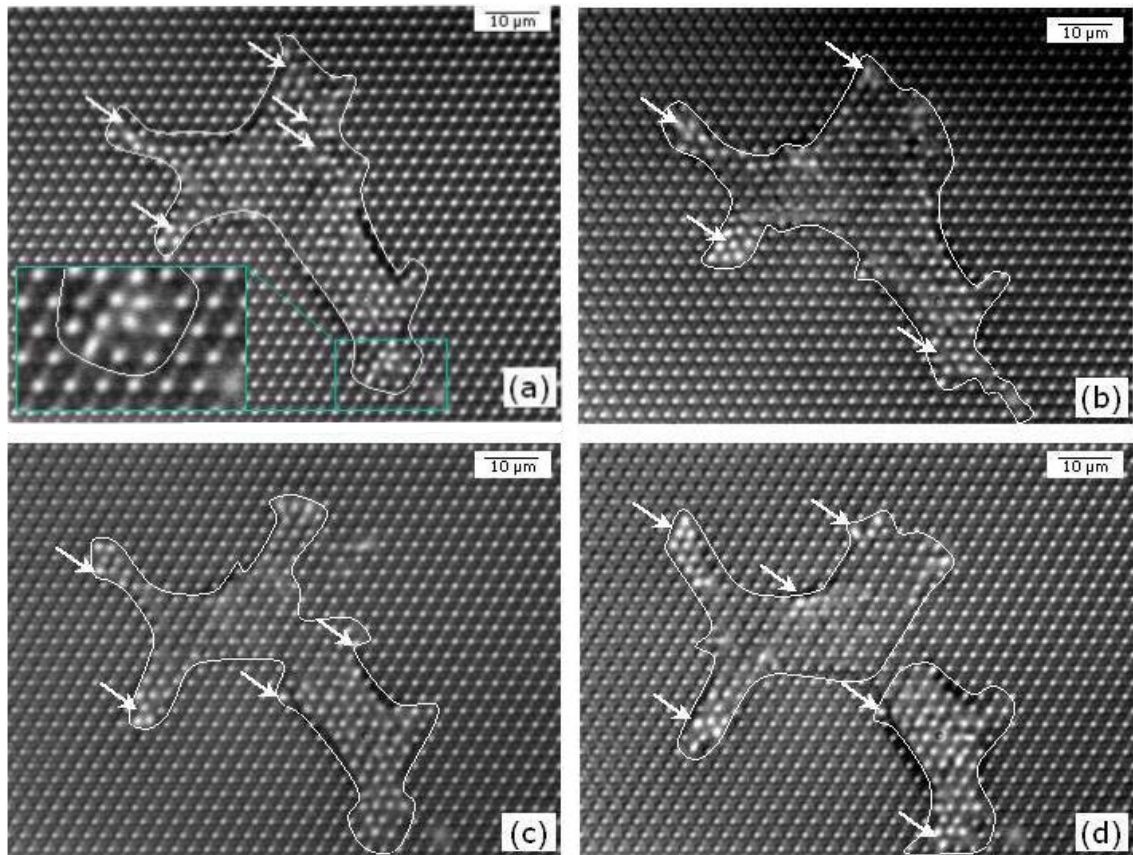


**Fig. 2.9. Deformation of micro pillar pattern under the effect of cell traction. These 4 phase-contrast images show the evolution during cell division. Small arrows represent the positions of several micropillars deformed from their equilibrium position in areas of "large deformations". Time interval between successive pictures is 20 minutes. The inset shows a zoomed region of the image (a) [33].**

The main limitation of this method is that rapid reproducibility of the devices is difficult. Since the microposts are directly in silicon any damage to it would require reproduction of the entire device again.

### C. Laser light diffraction methods and optical tweezers

The deformation characteristics of single cells obtained by laser light diffraction were first reported by Krueger et. al [36]. The striations observed in the sarcomeres as shown in Fig. 2.10 through microscopic imaging can be used to estimate the amount of forces exerted. If the stiffness of the cell is known the amount of displacement seen in the striations can be used to calculate the beating force of cardiomyocytes.

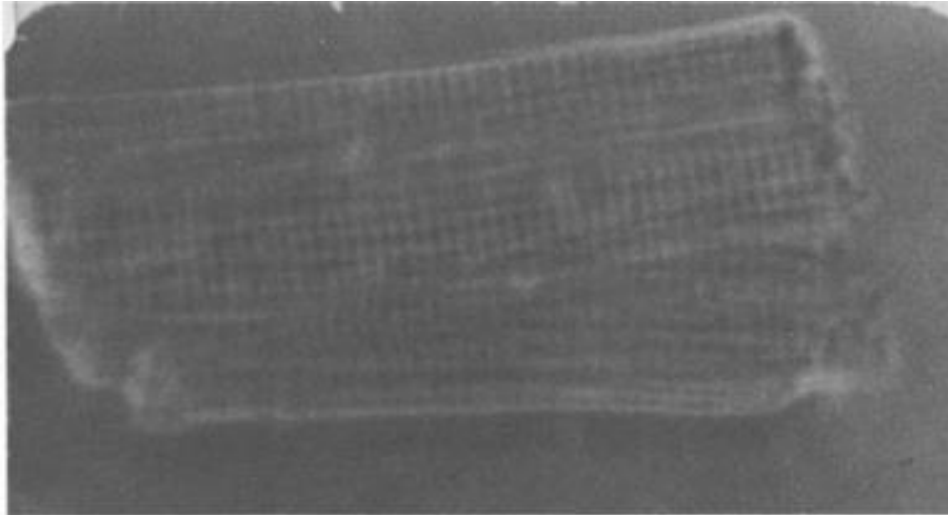


**Fig 2.10. Striations observed through microscopic imaging of cells using laser light diffraction as employed by Krueger et. al. [36].**

One main advantage of this method is that the approach permits real-time measurements of the sarcomere length at rest and during contraction. However, when applied to isolated cardiomyocytes, one main disadvantage of this method is that small volume of cardiomyocytes reduces the amount of optical grating, which results in a faint diffraction pattern. This can be overcome by increasing the laser power of the source but that also results in reduction in lifetime of the isolated cardiomyocytes [36]. To overcome this problem, Niggli [37] developed an optoelectronic device, which had a reduced susceptibility to optical noise, to record the sarcomere length of cardiomyocytes. This was a novel approach and led to improvement in sensitivity and reduction in optoelectronic power. Ivester et al.[38] developed a method to electrically stimulate cardiomyocytes to increase the protein synthesis rates. They used laser diffraction method to successfully observe the beating rates.

Laser beams have also been used in tandem with a dielectric bead as optical tweezers where optical forces have been used to tug and pull a sample cardiomyocyte creating linear forces. The bead surface is functionalized to bond with the cell surface. The high intensity laser beam creates an optical field which attracts the functionalized bead to its focus, thus generating a force which can deform the cell. Some groups have used this method to study elasticity of human erythrocyte [39,40] but there has not been any known attempts to measure the mechanobiological properties of cardiomyocytes. Also this method poses some limitations like possible photo damage due to the wavelength and power of the lasers.

### 2.3 Summary of the methods of force measurement

The literature review which was a major part of the thesis work helped to gain knowledge about the available methods of detecting beating forces in cardiomyocytes and choosing the most suitable method for implementation. AFM was chosen as the most suitable method as it is capable of detecting forces from the piconewton scale to the micronewton scale. Such a large range of force measurement ensures that the mechanical properties of cells measured with AFM can be validated with the measured values of other known standard samples like PDMS. In other words, if the Young's modulus of PDMS measured with the force distance spectroscopy mode of AFM corresponds to their known values, then a transition can be made to softer matter like cells to check if its Young's modulus can also be correctly reported with atomic force microscope. As PDMS is about several times stiffer than cells, so measurement of samples of different stiffness asserts the accuracy of the AFM in measuring a wide range of samples of varying stiffness. Once AFM was finalized as the method that will be used to measure the beating forces of cardiomyocytes, a novel manipulation of the AFM was implemented in which z axis of the piezo tube of the AFM as well as the cantilever was kept stationary to measure the beating forces of cardiomyocytes without any fluidic disturbances. The methodology and results is reported in details in the sections 4 and 5 of this thesis.

A summary of the results of chapter 2 involving different methods of force measurement and their suitability for measuring the beating force of cardiomyocytes is shown in Table 2.1. The list in section 2 is by no means exhaustive but highlights the most commonly used methods for measurement of cellular forces in cardiomyocytes. There are obviously certain challenges in this approach as the force might be too small to be measured. Moreover, the rhythmic patterns of beating might be different and can be irregular in case of a single cell.

**Table 2.1 Summary of methods and techniques for cellular force estimation**

Technique	Principle	Force Range	Suitability for single cell	Reference
<b>Atomic force microscopy</b>	Cantilever with nanoscale tip probes over cellular substrate to measure beating-forces as well as mechanical prop-	Piconewton to Micronewton range	Suitable	[7-10]

	erties.			
<b>Cell drum</b>	Cardiomyocyte placed on the cell drum silicon membrane to measure cellular pressure.	10 to 20 piconewtons to a few micronewtons.	Suitable	[12-19]
<b>Magnetic beads</b>	Tiny magnetic beads embedded in cells and manipulated by magnetic forces.	2 piconewtons to 100 nanonewtons	Suitable	[11]
<b>Carbon fiber based systems</b>	Carbon fibers attached directly to cell and controlled using feedback systems.	Less than 5 micronewtons. Lower limit not known.	Suitable	[20-21]
<b>Micro force sensors</b>	Has a probe which on coming in contact with the beating cell provides an output voltage proportional to the force	Upto a few millinewtons with a best possible resolution of 5 nanonewtons.	Not suitable as the resolution is more than the forces exerted by stem cell derived cardiomyocytes.	[22-27]
<b>Video imaging</b>	Frame by frame capture of cell position used to estimate forces	Any	Suitable.	[28-31]
<b>Flexible sheets</b>	Distortion in sheets used to estimate forces	Lower limit in a few hundred nanonewton range.	Not suitable as forces generated by single iPSC generated cardiomyocyte	[32-35]

			may not be enough to create distortions	
<b>Laser light diffraction.</b>	Powerful laser source focused on cell and from the laser diffraction forces can be estimated.	Upto a few micronewton.	Not suitable as this method reduces the life of a single cell drastically as well as optical noise is there.	[36-38]
<b>Use of laser beam as optical tweezers.</b>	Dielectric beads of high refractive index are moved using laser beams.	2 piconewton to 600 piconewton.	Not suitable as this method reduces the life of a single cell drastically.	[39-40]

Even though some of the methods listed above are suitable for force measurement in single cardiomyocytes, the ease of implementation of a method and the accuracy of reported data must be considered. The transducer-based methods are more accurate than the optical methods as they do not involve any approximations but rely on raw data. Amongst the transducer-based methods, the cell drum is only capable of reporting the total forces of the sample containing cardiomyocytes. For the other three methods given in Table 2.1, the range of force measurement is not as large as it is for an AFM.

### 3. AFM: THE MOST SUITABLE METHOD.

A more detailed study of the AFM is necessary at this stage. The main focus of this chapter is to familiarize with the basic concepts of AFM, its modes of operation, liquid cell imaging with temperature control, cantilever selection procedure, force distance spectroscopy and software provided with Park Systems XE-100 AFM.

#### 3.1 Atomic force microscope: basic concepts

The basic operation principle of an atomic force microscope was discussed in details in the section 2.1a of the thesis. Briefly, an AFM builds topographical images of sample surfaces by interaction of the cantilever tip with the sample. Once, an image is constructed, points can be chosen on this surface to determine mechanical properties of the sample surface using a force distance spectroscopy mode. These are the two key aspects of an AFM that are of relevance in this thesis even though the AFM can be used for a variety of other purposes like force volume spectroscopy, dynamic force microscopy, lateral force microscopy, I-V spectroscopy, etc. The AFM used for this thesis is the general purpose Park Systems XE-100. The XE-100 scanning probe microscope (SPM) system is made of three main parts: the XE-100 SPM stage, the XE-100 control electronics, and a computer with two monitors. A schematic diagram of the components of the SPM system is shown in Fig. 3.1.



**Fig. 3.1. The Park Systems AFM XE 100 SPM system.**

The scanning probe microscope is the main component of the system where the actual measurements are made, the video monitor which displays the image from the optical microscope indicate the exact spot on the surface where imaging is to be done and al-

so spots the cantilever, and the XE 100 Control Electronics controls the movement of the SPM stage according to instructions from the computer.

### 3.2 XE 100 SPM stage

The XE 100 SPM stage is enclosed in an acoustic enclosure to eliminate noise and housed over a stone table and anti-vibration platform to eliminate vibrations. The main components of the scanning probe microscope are the XE 100 head, objective lens, XY scanner, XY stage, Z Stage, optical microscope and CCD camera as shown in Figure 3.2. The figure labels all the individual parts of the SPM stage.

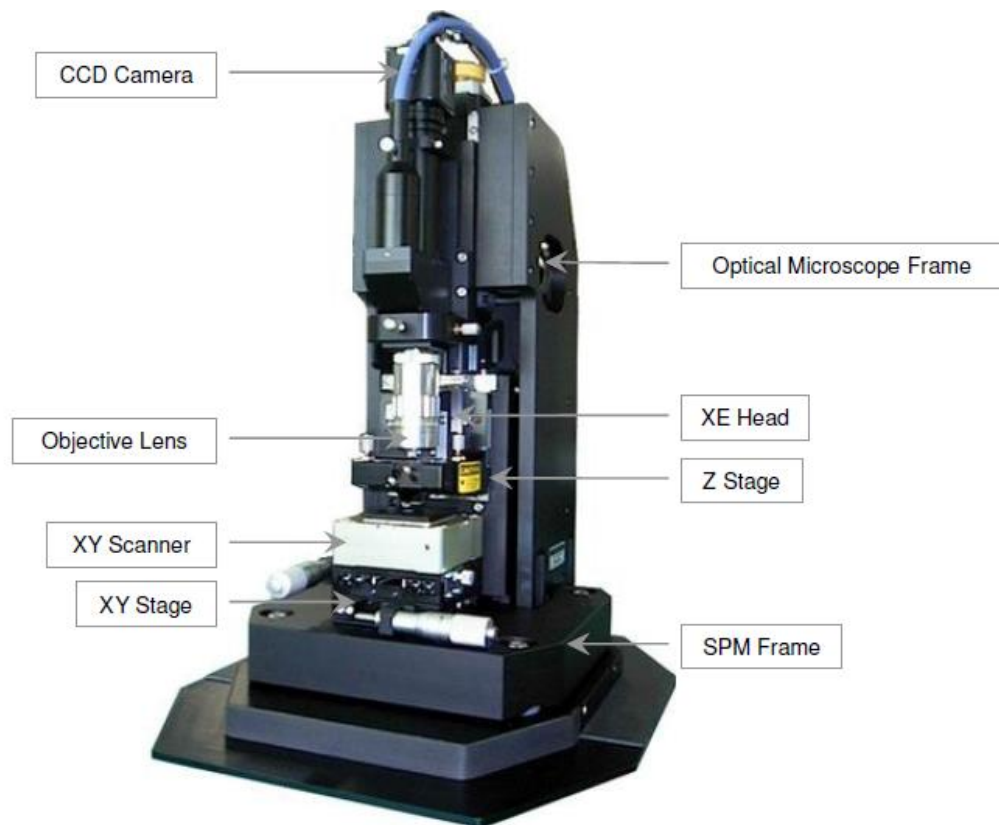


**Fig 3.2. A Schematic Diagram of the XE 100 SPM stage [43].**

The XE 100 head is the component, which carries the cantilever probe and interacts with the sample. The Z stage controlled by the control electronics is used for lowering the head onto the sample. The Z scanner housed on the XE 100 head has a range of 12 micrometers and is capable of constant feedback conditions as the head moves towards the sample surface. The XY stage and scanner moves the sample horizontally. The CCD camera coupled with the optical microscope takes images of the sample as seen with the optical microscope with 10X objective lens. The probe's movement is detected to construct a topographic image by gathering the laser beam signal on a

PSPD (Position-Sensitive Photo Detector) after it is reflected from the back side of a cantilever. Laser alignment is executed with easy to manage control knobs on the XE-100 head. Additionally with the help of the control software and the video monitor display, the spotting and movement of the laser beam becomes convenient and precise. The tip wears out after some time and the replacement of tip is convenient with the kinematic mount on XE 100 head. The optical microscope is used to focus the laser beam above the cantilever and also displays interesting region on the sample surface that is to be imaged. Since the optical microscope is mounted alongside with the Z-scanner, it is possible to have a direct on-axis view of the cantilever in conjunction with the sample area that is to be scanned.

### 3.3 Modes of operation

The interaction between the probe tip and the sample can take place in three modes: contact, non-contact and intermittent modes, the last one known also as tapping mode. In contact mode the AFM probe softly scans over the sample surface, and using the repulsive force that is exerted vertically between the sample and the probe tip then generates an image of the sample's topography. Although the interatomic repulsive force between the sample and the probe tip is merely 1~10 nN, the spring constant of the cantilever is also very small (less than 1 N/m), thus enhancing the possibility of the cantilever to capture very small forces. The AFM detects even the tiniest amount of a cantilever's deflection as it moves across a sample surface. Thus, when the cantilever scans a convex area of a sample, there is an upward deflection, and when it moves over a concave area, there is a downward deflection. This probe deflection is used as a feedback loop input that is sent to an actuator (z-piezo). The cantilever deflection recorded is used to construct an image of the sample surface as it is probed.

During the cantilever tip and sample interactions, there are two main forces, the static electric repulsive force and attractive force, present between atoms a short distance apart. When the distance between the atoms at the end of the probe tip and the atoms on the sample surface becomes much shorter, the repulsive forces between them become dominant, and the force change due to the distance change becomes greater and greater. Therefore, contact AFM measures surface topography by utilizing the system's sensitive response to the repulsive Coulomb interactions that exist between the ion cores when the distance between the probe tip and the sample surface atoms is very small.

However, as shown in Figure 3.3, when the length between the probe tip and the sample surface is relatively more, the attractive forces come into play and dominate. Ion cores become electric dipoles due to the valence electrons in the other atoms, and the force induced by the dipole-dipole interaction is the van der Waals force. Non-contact AFM (NC-AFM) measures surface topography by utilizing this attractive atomic force in the relatively larger distance between the tip and a sample surface [8].

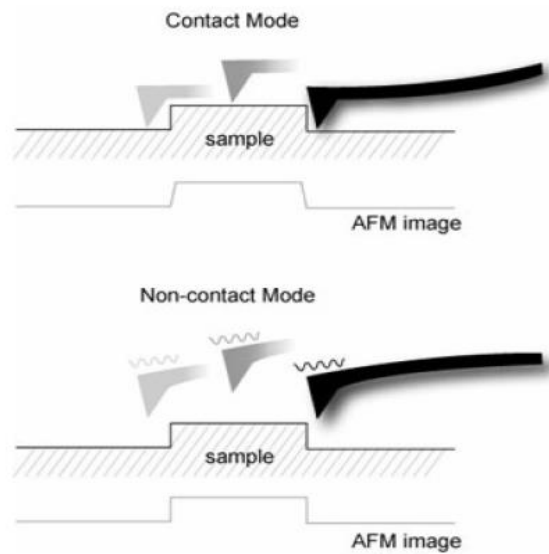


**Fig. 3.3. Concept diagram of contact and non-contact modes of imaging [8].**

Figure 3.3 shows the movement of the probe tip with respect to the sample surface giving a comparison between contact AFM and non-contact AFM. Contact AFM involves the probe tip contacting physically the sample surface, while noncontact AFM does not come in contact with the sample. In non-contact mode, the force between the tip and the sample is very weak so that there is no unexpected change in the sample during the measurement. Thus, non-contact AFM is very useful for cells or other soft matters measurement; with the tip also lasting longer. On the other hand, the force between the tip and the sample in the non-contact regime is very low, and it is not possible to measure the deflection of the cantilever directly. So, non-contact AFM detects the changes in the phase or the vibration amplitude of the cantilever that are induced by the attractive force between the probe tip and the sample while the cantilever is mechanically oscillated near its resonant frequency. The intermittent contact mode is somewhat in between these two modes and makes occasional contacts with the sample surface and possibly covers up for the deficiencies of both the modes. So, if it is necessary to image as well as probe the mechanical properties of soft samples like cells, this can be the most suitable mode. In intermittent mode the cantilever oscillates at or slightly below its resonant frequency. The amplitude of oscillation generally varies from 20 nm to 100 nm. The cantilever gently taps on the sample surface during scanning, contacting the surface at the bottom of its swinging cycle. Since, the forces on the tip change as the tip to surface distance changes, the resonating frequency of the cantilever depends on this distance.

### 3.4 Liquid cell imaging

The Park Systems XE-100 AFM comes with a liquid cell designed especially for carrying out sample measurements in the liquid medium. The liquid cell comes with a probe holder known as "liquid probe hand" used for holding the cantilever with the nanoscale tip. The liquid probe hand is designed especially for working in liquid environment and is different to the multiclip probehand used in air, which presents a danger of short circuiting the electronic circuit of the XE 100 head if used in liquid. The universal liquid cell and the liquid probe hand are shown in Figure 3.4.

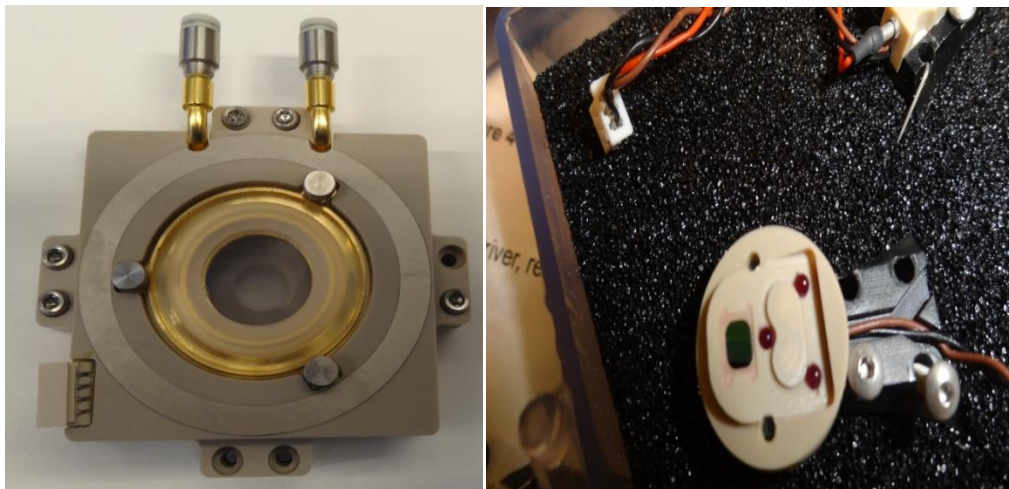


**Fig. 3.4. The universal liquid cell and the specially designed liquid probe hand.**

The universal liquid cell can be used both as an open liquid cell and a closed liquid cell, where the additional advantage of controlling the temperature from 0 °C to 70 °C is present with a temperature resolution of 0.1°C. The capacity of liquid is 3 cm<sup>3</sup>. It is capable of holding a sample size of 20 mm in diameter or 5 mm in thickness. It comes with a compatible probe hand: the shielded liquid probe hand as discussed earlier and a compatible 50 μm XY-scanner.

### 3.5 Cantilever selection procedure

Many types of cantilevers can be used and they vary in material, shape, softness (shown by the spring constant), intrinsic frequency, and Q-factor. The choice of the cantilever primarily depends on the mode of measurement and the type of sample to be measured. For measuring a biological sample in the contact mode, a soft cantilever, having a lower spring constant in the range of 0.01 N/m ~ 3 N/m is needed to react appropriately to the small force between atoms. The probe cantilever used in the contact mode is about 1

micrometer thick so that a small spring constant can be achieved. The reason behind this is a cantilever with a low spring constant makes a relatively bigger deflection to a small force, and thus gives a very detailed image of the surface topography. On the other hand, in non-contact mode, a cantilever is thicker, about 4 micrometer. The spring constant range in non-contact mode is 3 to 75 N/m with a nominal range of 25 to 40 N/m, which is very “stiff”, and a relatively large resonant frequency. Whereas contact mode measures the bending of a cantilever, the non-contact mode vibrates a cantilever at a high resonant frequency, and measures the force gradient by the amplitude and phase change due to the interaction between the probe and the sample, which yields the topography of the sample. If the probe tip is sharp the surface area of the tip and surface tension is low and leads to a more stable operation. This is because when operating with soft samples there are chances that traces of soft matter stick to the tip due to surface tension. There are more chances of this happening if the spring constant of the cantilever is smaller which will also make it difficult to bring the probe back to its original position. Thus a higher spring constant is needed to overcome the surface tension in non-contact mode. For dealing with soft samples like cells in liquid medium, the spring constant of the cantilever should be below 1N/m.

### **3.6 Force distance spectroscopy**

Even though the AFM is best known for its high-resolution imaging, it is also a powerful tool for measuring tip sample interaction forces. This is the property exploited in this thesis to gain knowledge about the elasticity of the cardiomyocytes. The interaction forces experienced by the cantilever as it approaches from several microns above the sample can give an idea about long-range electrostatic forces. When the tip sample distance is about a few tens of nanometers, the attractive van der Waals forces come into play. At very short tip sample distance, the attractive forces overcome the repulsive electrostatic forces leading to an overall attractive force which may lead the tip to jump into contact with the surface, an effect known as "snap in". Once the cantilever has made contact with the surface, it may be pushed onto the surface with some force to find out the viscoelastic properties of the surface as well as the Young's modulus and stiffness of the surface. When the cantilever is pulled away from the surface, adhesion forces can be measured and the molecules sticking between the sample surface and tip are stretched. An overview of the tip sample interaction measured at different points during a force spectroscopy cycle is shown in the Fig.3.5.

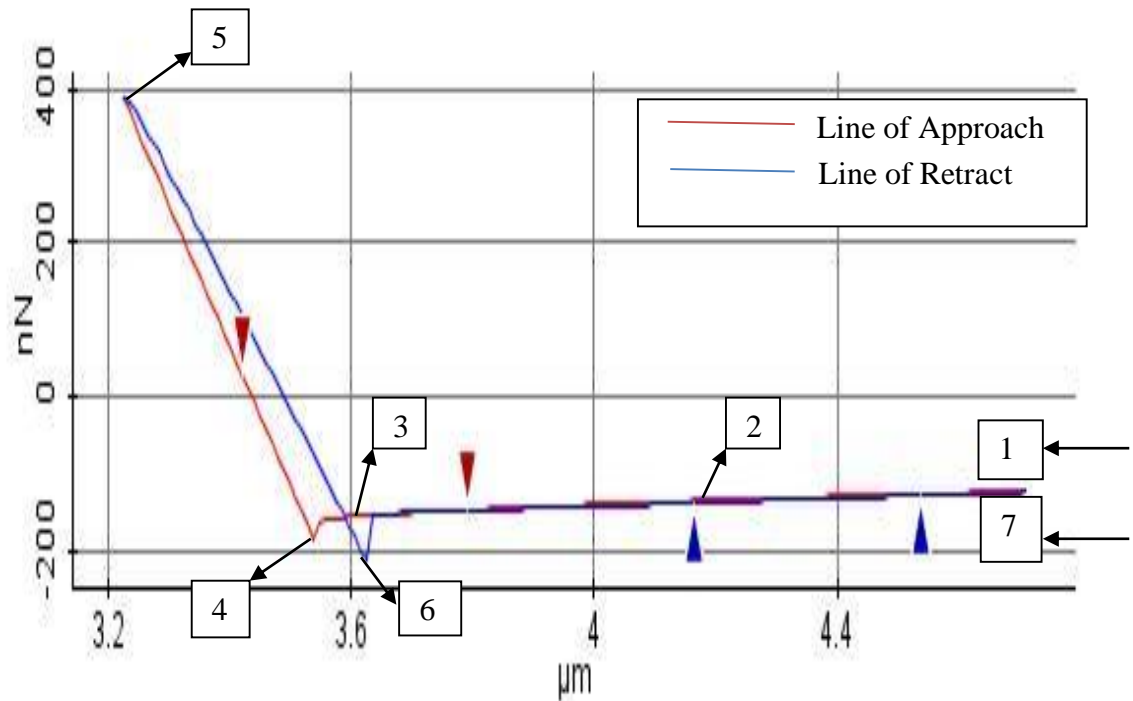


**Fig. 3.5. Overview of interactions measured at different points during a sample force spectroscopy cycle with red arrows pointing downwards showing the line of approach and blue line pointing upwards showing the line of retract. A positive slope denotes an attractive force and a negative slope denotes a repulsive force.**

The different points from 1 to 7 mark the different phases of the force spectroscopy cycle. At point 1, the tip is 10 to 100 microns away from the sample and there are no interaction forces which means the force is zero nanonewtons. Point 1 does not lie in the area of the figure and is thus shown with an incoming arrow, which means it is at a far off distance. The tip starts approaching towards the sample now and at point 2 is a few microns away from the sample. At this the electrostatic forces and long-range interactions from adsorbed molecules come into play and it can be seen from the figure that the resultant of these forces is attractive in nature. The tip gets even closer to the sample with the distance of separation being a few nanometers at point 3. At this stage, the Van der Waals' forces, capillary forces in air and screened electrostatics in aqueous solutions dominate over the repulsive forces pulling the tip towards the sample, an effect known as snap in. Point 4 shown in the figure is the snap in point where the tip makes contact with the sample. At point 5, the tip is indenting the sample and mechanical properties of the sample like elasticity, Young's modulus, viscoelastic response as well as active forces like the beating force of cardiomyocytes can be extracted. After this point, the tip starts retracting from the sample. The red line in Fig. 3.5 above shows the line of approach of the tip towards the sample and the blue line shows retraction of the tip from the sample. Point 6 shows the point when the tip lifts off from the sample. At this point, the adhesion forces due to cell surface interaction with the tip can be seen. As such the

tip needs to apply some force to lift up from the surface. When a functionalized tip is used, then point 6 also denotes the ligand receptor adhesion forces. After this the tip breaks contact from the surface and keeps moving away from the surface such that the stretched molecules between the tip and the surface break and at point 7 there is no further interaction which means the force is zero nanonewtons. Again, point 7 does not lie within the figure and is at a distance of some tens of micrometers from the sample; hence it is shown with an incoming arrow. As it's seen in the description above, the beating forces of the cardiomyocytes is measured from the force data available at point 5 of the cycle. It denotes the tip sample maximum repulsive interaction force.

### **3.7 XE 100 software**

The Park Systems XE-100 AFM comes with three software: the camera software XEC, the data acquisition software XEP, and the image processing software XEI. The positioning of the tip, the control of the AFM and the processing of the obtained images and results are done by means of these three software. Hence this section is devoted to a more thorough understanding of the three software and the parameters that are used during imaging and force measurements.

#### **a. Camera software XEC**

XEC is the Park Systems XE-100 AFM camera software which allows the user to see the optical microscope image taken by the CCD camera. Also, it is useful for seeing the cantilever approach the sample surface and gives a view of the sample surface as well. It enables to find out the interesting area to image on the sample as it gives a good view of the sample surface. The software also allows zooming to the surface and this gives an additional camera zoom in addition to the optical microscope 10 X zoom. It also helps to find out the laser spot on the cantilever before the Z stage is lowered onto the sample. It has some other features too like grabbing a snapshot of the sample surface and placing a crosshair, which helps to locate the cantilever, as shown below in Fig 3.6.

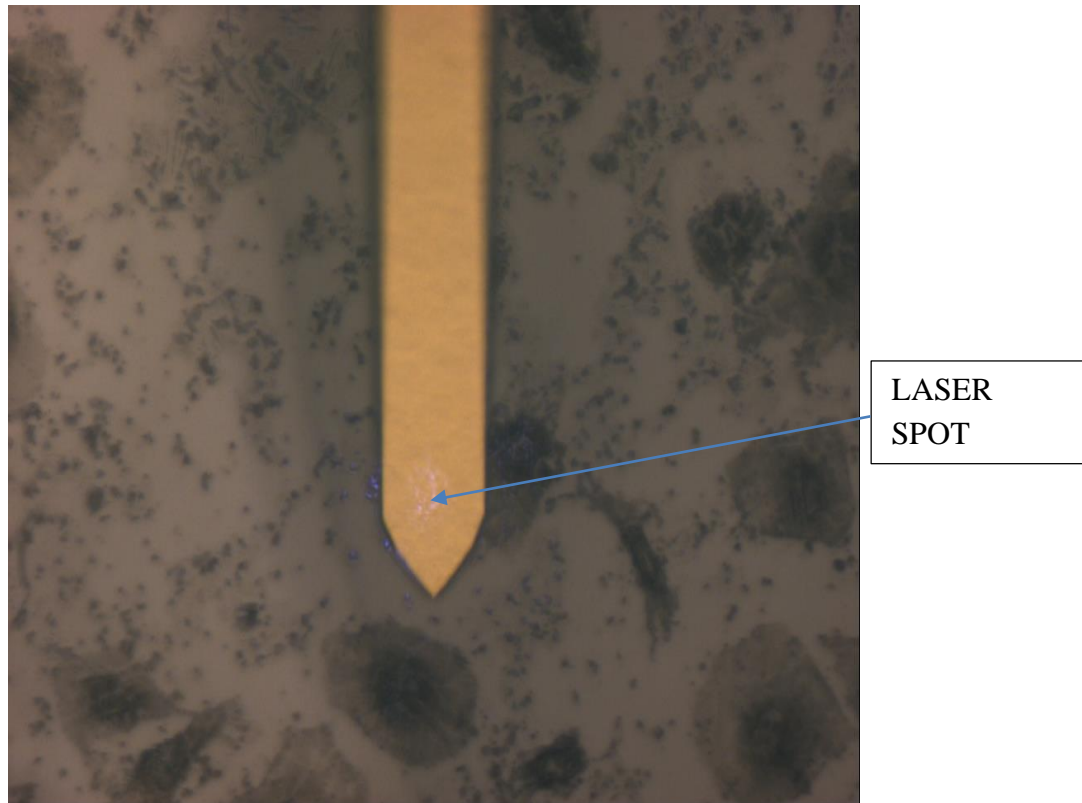


**Fig. 3.6.** A grabbed snapshot of the XEC software with a view of the cantilever on the sample surface containing fixed END-2 cells.

### **b. Data acquisition software XEP**

The data acquisition software XEP is responsible for operating and controlling the Park Systems XE-100 AFM. It has a huge number of features but here the discussion is restricted to the features most necessary for imaging and force distance spectroscopy measurements. The XEP software user interface is divided into several windows as shown below in Fig. 3.7.

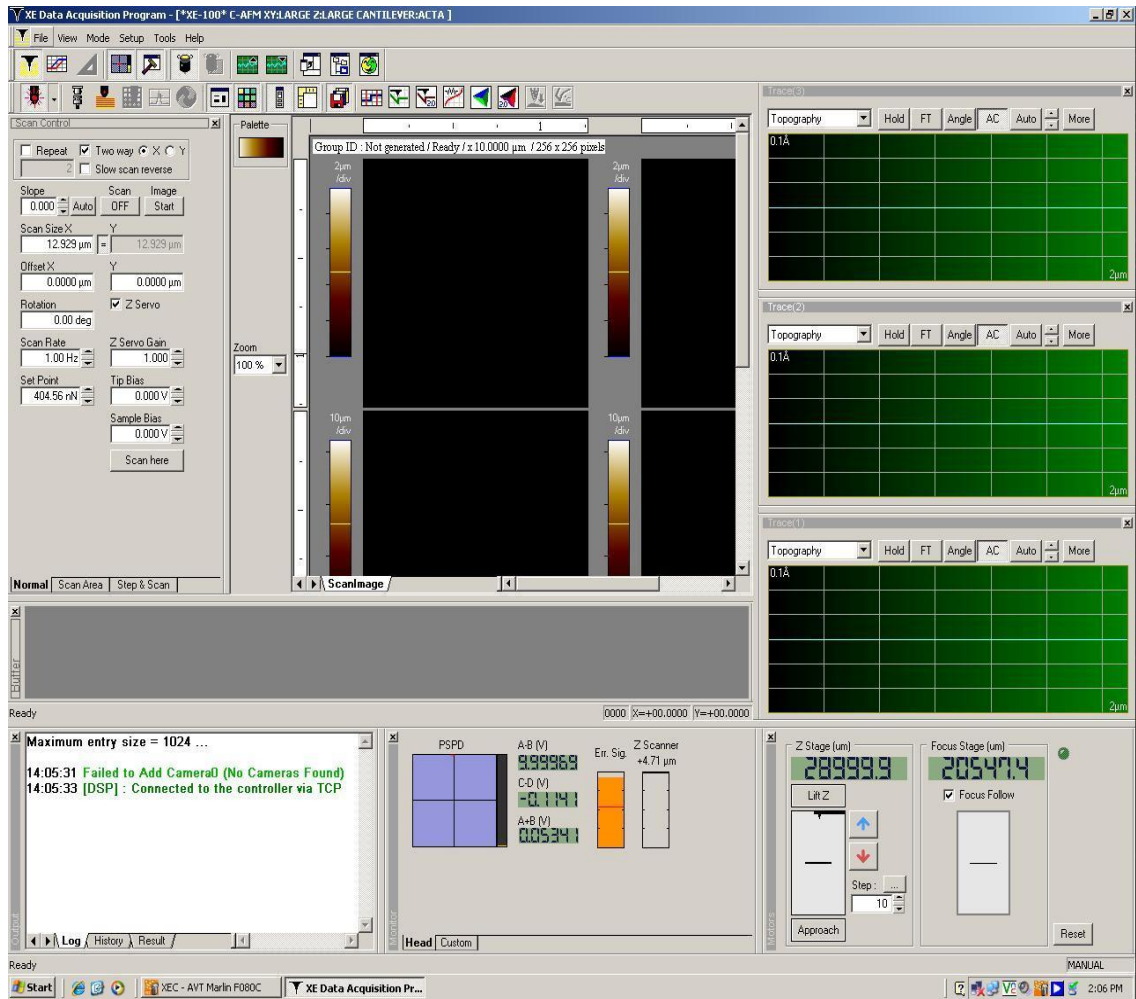


**Fig. 3.7. Park Systems XE100 XEP data acquisition software user interface.**

The different windows on display above are described one by one below along with a short description of the FD spectroscopy mode and nano indentation mode. The scan control window is necessary for setting up a scan and taking an image. The scan size helps in setting the area of scanning. A scan size of X equal to 12 micrometers means a scan area of 12 micrometers by 12 micrometers. Signals shown on the oscilloscope screen are obtained along the scanning direction. A yellow trace line on the Oscilloscope screen shows the signal obtained from the forward scan direction. If the backward scan direction is selected from the "Input Configuration window", a blue trace line will also be displayed on the screen. For good imaging, the blue and the yellow line should follow each other nicely in three windows: Amplitude, Phase and Topography. When this condition is met imaging can be started. The Z stage position and the focus stage values are shown in the Stage Control windows. They help to find the position to take an image and helps to follow the position of the tip with the optical microscope, respectively.

Before proceeding to force distance spectroscopy it is very important to take an image of the sample in the scan mode. Even a half image or any partial image of the sample is

alright as long as the user has a good idea of the topography of the sample and knows which portions of the sample to measure.

In force distance spectroscopy mode, a short description of some parameters is necessary to complement on the knowledge gained in section 3.6. The parameters, Z highest and Z lowest in force distance spectroscopy mode are used to limit the maximum distance the tip can penetrate into the sample. Down Speed and Up Speed are used to control the rate of approach of the tip towards and away from the sample respectively. The setpoint is used to range in which the force applied by the tip on the sample should be and it can be 40 to 70 per cent of the force limit. Force limit is the limiting or absolute value of the force exerted by the tip on the sample and if it exceeds beyond that then the cantilever might be damaged. Normally, each and every type of cantilever has its own force limit and setpoint values depending on its specifications. As the specifications of the cantilever are fed in the XEP software part database, the FD Spectroscopy mode is able to calculate by itself the maximum value of the force limit. If the user tries to put a higher value than calculated by the software, it stops at the maximum force limit value calculated by the software (see Appendix).

### **c. XEI image processing software**

The Park Systems XEI image processing software is again a software with a huge number of features like the data processing software. However, here we keep our discussion limited to the most essential features of the software necessary from the point of view of the thesis.

A three dimensional image of the topography can be seen in the image processing software. The information section of the software gives a complete overview of the parameters used during imaging for example, information about the cantilever, date of imaging, mode of imaging, scan rate during imaging, Z Servo gain and area of the image. There is a separate button for selecting the force distance spectroscopy mode and that gives information on the force distance curves obtained at all the selected points in the topography of the image. Several such force distance curves were needed during the course of the measurements to have an idea about the elasticity of samples as well as for measuring the beating force of cardiomyocytes.

## 4. METHODS AND MATERIALS

This chapter deals with the sample preparation methods for the cell samples as well as the reference PDMS samples, which were measured for topography and force distance measurements. Also, the principle of calculating the Young's modulus from the force distance spectroscopy curves is presented in this chapter.

### 4.1 Sample preparation method: Beating cardiomyocyte and fixed non beating cardiomyocyte.

The Heart Group of BioMediTech, University of Tampere, prepared the cell samples. For the purpose of our study, mouse visceral endoderm like (END-2) cells were used to induce cardiac differentiation of hiPSCs [43]. Human iPSCs were maintained in an undifferentiated state on the top of mitomycin C treated mouse embryonic fibroblast (MEF) feeder cell layers (26000 cells/cm<sup>2</sup>) (Millipore Corporate). The culturing medium for hiPSCs was KSR-medium [Knockout DMEM (Invitrogen), 20% knockout serum replacement (ko-SR, Invitrogen), 2 mM Gluta Max (Invitrogen), 1% non-essential amino acids (NEAA, Lonza), 50 U/ml penicillin/streptomycin, 0.1 mM 2-mercaptoethanol (Invitrogen) and 4 ng/ml basic fibroblast growth factor (bFGF, R&D Systems)]. hiPSCs were enzymatically passaged with type IV collagenase (1 mg/ml, Invitrogen) once a week. An image of undifferentiated hiPSC cells on MEF feeder colonies is shown in Fig.4.1.

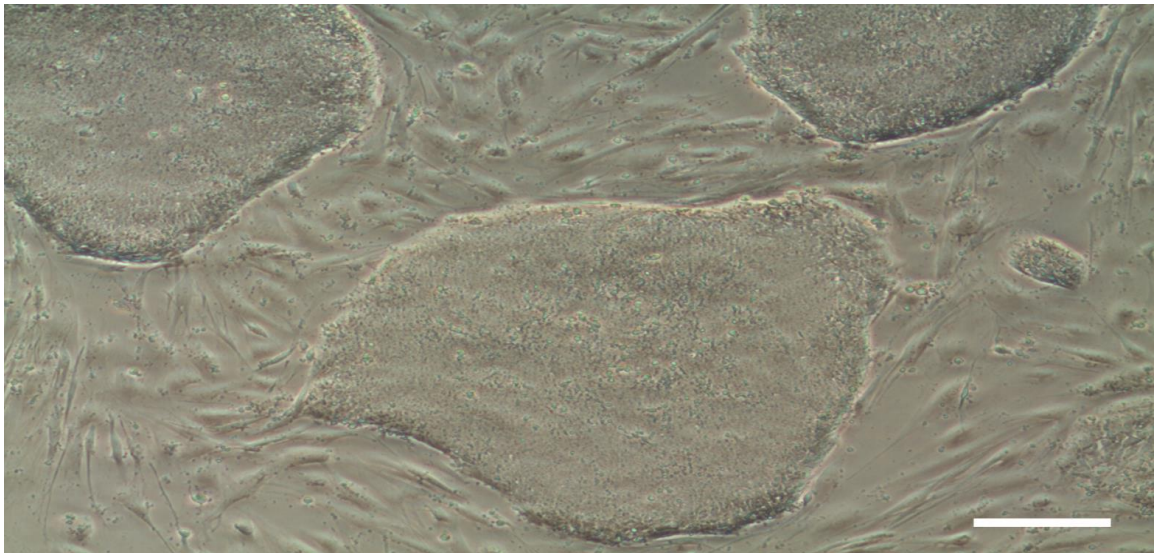


**Fig. 4.1. Undifferentiated hiPSC colonies on MEF feeder cells with a 10x optical microscope and scale bar 200  $\mu$ m.**

To initiate the cardiac differentiation, hiPSCs were co-cultured with Mitomycin C (Sigma-Aldrich, St. Louis, MO, USA) treated END-2 cells (50000 cells/cm<sup>2</sup>) in KSR medium without ko-SR or bFGF and supplemented with 3 mg/ml ascorbic acid (Sigma-

Aldrich). Medium was changed after 5, 8 and 12 days of culturing. At day 14, 10% ko-SR was included and ascorbic acid was excluded from the culture medium, and changed 3 times a week. After 15 days of culturing, cells formed beating clusters in END-2 co-cultures as shown in Fig.4.2.

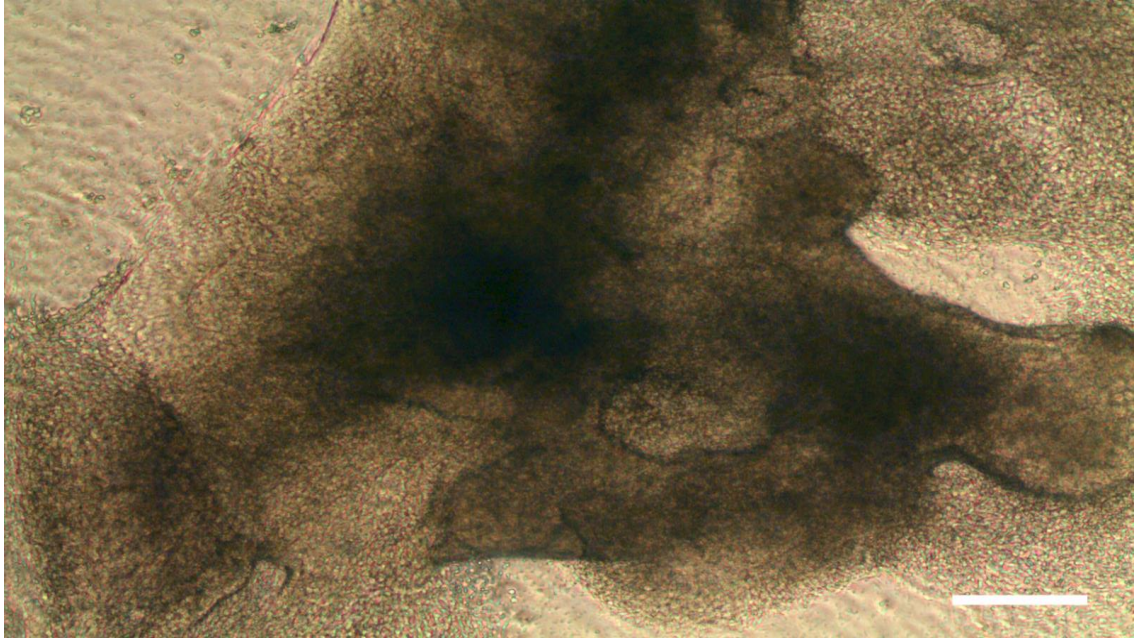


**Fig. 4.2. hiPSCs in End 2 co-cultures prepared by BioMediTech with a 10x optical microscope and scale bar 200  $\mu\text{m}$ .**

Beating cell clusters were cut out manually by scalpel and dissociated into a single-cell suspension using Collagenase A (Roche Diagnostics GmbH, Mannheim, Germany) treatment [44]. Dissociated cells were plated onto 0.1% gelatin coated cover slips of 25 mm diameter.

At first, the force measurements were carried out from fixed cell samples to practise the AFM method. END-2 cells or dissociated cardiomyocytes were fixed with 4% para-formaldehyde (Sigma-Aldrich) at room temperature for 20 min. Samples were stored in PBS at +4°C until the AFM experiments. The force measurements were carried out in PBS. Next, the force of beating cardiomyocytes was measured. The force measurements of beating cardiomyocytes were carried out at +37°C in a liquid consisting of (in mmol/L): 137 NaCl, 5 KCl, 0.44 KH<sub>2</sub>PO<sub>4</sub>, 20 HEPES, 4.2 NaHCO<sub>3</sub>, 5 D-glucose, 2 CaCl<sub>2</sub>, 1.2 MgCl<sub>2</sub> and 1 Na-pyruvate (pH was adjusted to 7.4 with NaOH).

## 4.2 Sample preparation method: PDMS structures

The Microsystem Technology group at the Department of Automation Science and Engineering, Tampere University of Technology provided six PDMS structures. PDMS has a Young's modulus of typically around 1 to 2 MPa depending on the mixing ratio of base to curing agent. So, this means that it is only about 10 times more stiffer than cardiomyocytes which has Young's Modulus in the range of 100 KPa [9,10,46]. As such it was an ideal material to validate the measured forces. In other words, if the measured Young's modulus of the PDMS samples corresponds to the known stiffness values then it is a good testimony to the fact that the AFM is suitable for accurate force measurements.

Microfluidic chips were fabricated using the standard soft lithography technique:

(a) A 4-inch silicon wafer was spin-coated with negative photoresist (SU-8, MicroChem Inc., thickness target: 1 to 5  $\mu\text{m}$ ), and then the coated silicon wafer was soft-baked for several minutes. The wafer was exposed under a mask using an aligner and placed on a hot-plate for several minutes of post-exposure baking, followed by a short relaxation time. Post-exposure baking was followed by development at room

temperature, after which the whole wafer was rinsed with isopropyl alcohol (IPA) to clean the residues

from the wafer. Subsequently, SU-8 was patterned on the first SU-8 layer

(b) A Polydimethylsiloxane (PDMS) precursor (Sylgard 184 silicone elastomer, Dow Corning) and a curing agent were mixed at a ratio of 10 to 1, based on weight. Before the PDMS mixture was poured onto the fabricated master, the master was silanized with (tridecafluoro-1,1,2,2,-tetrahydrooctyl)-1 trichlorosilane to allow easier removal of the PDMS after curing. The PDMS mixture was poured onto the master and cured at 95  $^{\circ}\text{C}$  for 1 h.

(c) Then, the cured PDMS channel was peeled off from the master, cut and punched to connect microtubes.

(d) The PDMS devices were treated with oxygen plasma under 50 sqcm of O<sub>2</sub> and at a power of 70 W for 40 s. and then directly bonded to a glass substrate without any surface treatment. Tip sample interaction forces of the tip to PDMS sample as well as elasticity of the sample were successfully measured and are given in the results section of the thesis.

## 4.3 AFM probing of cell elasticity and interaction forces

The interaction between the sample surface and the tip (probe) of the AFM positioned very near to it relates to the force between the atoms present in sample and those of the tip that scans its surface. The approach of the tip to a nanometer range of the sample causes bending or twisting of the cantilever in a manner proportional to the interaction

force between them. The popular AFM method for quantitatively studying mechanical characteristics of cells and tissues is the force spectroscopy also known as force-curve analysis. Sufficient details of the basics of force distance spectroscopy and the software implementation of force distance spectroscopy mode were depicted in chapter 3. The force distance spectroscopy curves give information about the tip sample interaction force value and vertical deflection of the cantilever. The force curve contains information about long- and short-range interactions and represents a basis for estimation of sample's Young's modulus. Most popularly, the Hertz model as mentioned in [8] has been used for the calculation of Young's modulus of cells.

There are two important assumptions in the Hertz model, which describes the case of elastic deformation of two homogenous smooth bodies. Firstly, it assumes a parabolic shape of the indenter and secondly the indented sample is comparatively much thicker than indentation depth. The first assumption also remains valid for the case when a spherical tip radius is assumed and it is much bigger than the indentation depth ( $h < 0.3R$ ) [46].

When the tip of an AFM is assumed to be a sphere of radius  $R$ , then the tip sample interaction force on the cantilever is given by  $F(h)$  which according to equation 4.1 is:

$$F(h) = 4 \times \left(\frac{\sqrt{R}}{3}\right) \times E' \times h^{1.5} \quad (4.1)$$

where  $E'$  is the effective modulus of a system tip sample, and  $h$  is the depth of the indentation or in other words the precise vertical distance the cantilever travels from the moment it starts experiencing long range interaction forces.

The effective modulus in the case when the material of the tip is considerably harder than that of the sample is given by

$$E_{sample} = E' * (1 - \nu^2) \quad (4.2)$$

Where  $E_{sample}$  is the actual Young's modulus of the sample and  $\nu$  is the Poisson's ratio of the sample. For the measurements, Eq. 4.2 is used to find out the Young's modulus of the fixed dead cardiomyocytes samples [45]. If the displacement of the tip of the cantilever can be observed, then the force of the beating cardiomyocytes can be calculated by multiplying the displacement directly with the stiffness constant of the cantilever. The cantilever used for the measurements was Mikromasch HQ:CSC17/A1 BS having a minimum force constant of 0.06 N/m, typical resonance frequency of 13 kHz, 450  $\mu\text{m}$  in length, 50  $\mu\text{m}$  in width and 2  $\mu\text{m}$  in thickness.

When the data is obtained from the XE 100 software, it requires certain deal of processing to find out the beating forces. First of all, the data is obtained as negative values which have to be converted to positive values and the maximum negative value (or minimum positive value) is subtracted from each of these values to get the displacement at that point. Normally, the data from the XE 100 software is reported as a series of 510

points. After this step, we have the beating displacement at each of the 510 points. Now this beating displacement is multiplied with the spring constant of the cantilever to get the beating force. Once the beating force is obtained, the peaks of the data are identified and the maximum peaks are selected by specifying the value of the minimum peak. For example, if there is a series of peaks 0.1, 0.2, 0.15 and 0.07, then the minimum amongst these peaks is 0.07. A formula in excel is fitted to identify a local maxima first and then deliver the values of each of these maximas greater than the threshold value (0.07 in the above example which is obtained by visual inspection of the scatter diagram). A visual inspection of the scatter diagram is necessary to identify the threshold which is the minimum value of the peak as there can be some stray local maximas due to certain disturbances like noise and such local maximas do not need to be taken into consideration. Once, these local maximas are identified, an average of each of them is taken to report the average peak to peak beating force in one sample measurement. The calculations were carried out in Excel 2013.

## 5. RESULTS AND DISCUSSION

In this chapter, the results of the measurements are presented. PDMS samples, END 2 cells, fixed cardiomyocytes and finally beating cardiomyocytes samples were imaged and tested in force distance spectroscopy mode.

### 5.1 PDMS sample imaging and Young's modulus calculation

PDMS samples having groove like structures (as discussed in section 5.1) were imaged and the height and width of the grooves were validated with the AFM measurements as shown in Figure 5.1. The measurements were carried out in PBS solution, the same solution used as liquid medium for End 2 cells and fixed cardiomyocytes.

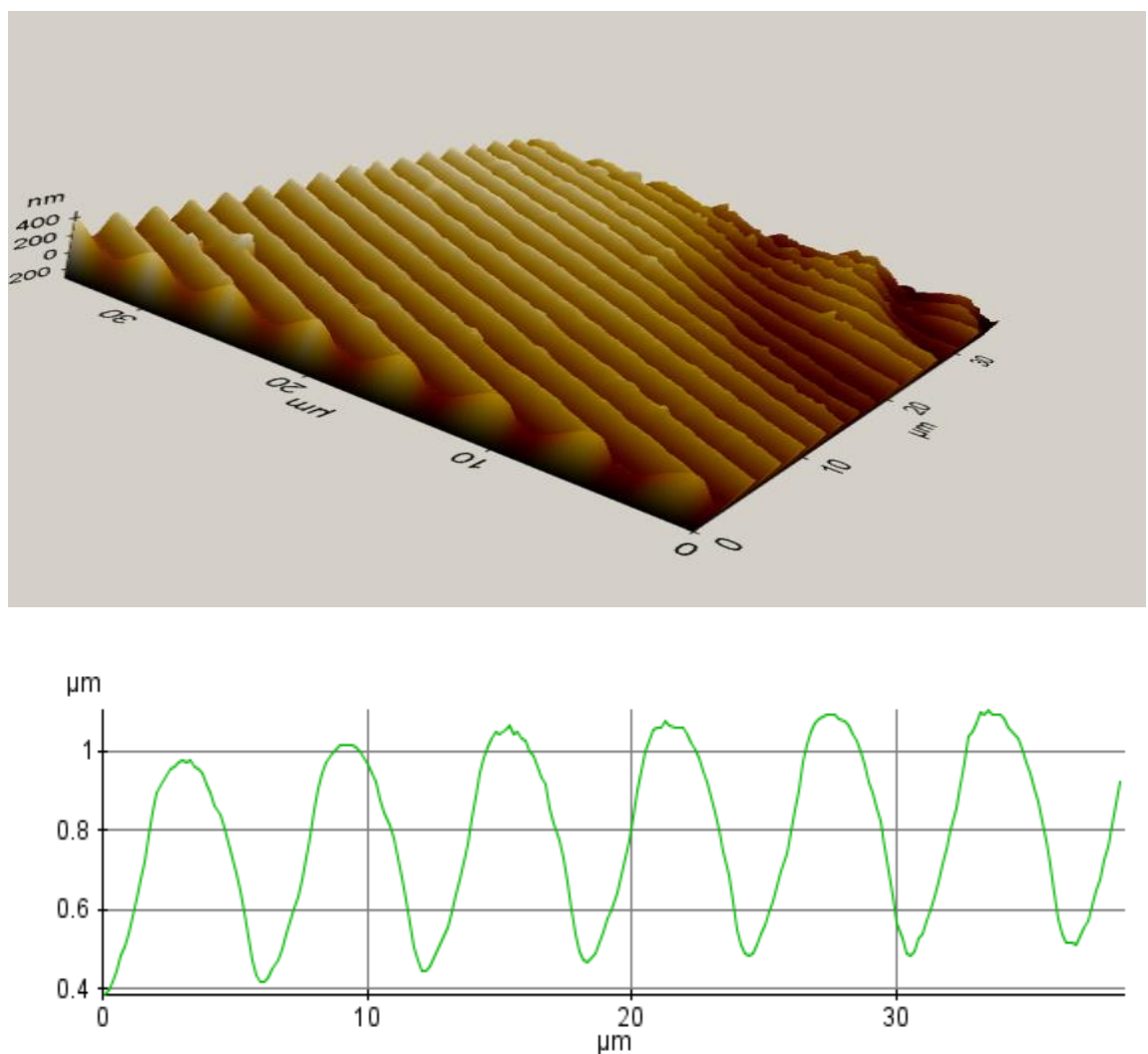


**Fig. 5.1. Sample PDMS structure with 1 μm high and 5 μm wide grooves imaged with AFM.**

As it can be seen from Fig 5.1, the dimensions were approximately  $1\ \mu\text{m}$  high and  $5\ \mu\text{m}$  wide. The width of the grooves is actually the peak to peak distance along the direction of groove as seen in the line profile of the topographical surface above in Fig. 5.1. For imaging PDMS samples in liquid, the intermittent mode of imaging was selected. The scan rate was kept low at  $0.2\ \text{Hz}$ , Z servo gain was  $6.5$  and the scan size was  $40\ \mu\text{m}$  by  $40\ \mu\text{m}$  in the XY direction. ACTA cantilever, which are silicon probes designed for non-contact, tapping mode, intermittent contact, and/or close contact applications, were used for the measurements. These probes have a high frequency that allows for faster scanning speeds, and have Aluminum coating on the reflex side to increase laser signal quality. The cantilever had a stiffness constant of  $25\ \text{N/m}$ , had a length, width and thickness of  $125\ \mu\text{m}$ ,  $45\ \mu\text{m}$  and  $4\ \mu\text{m}$  respectively. The resonant frequency of the ACTA cantilever in air was  $310\ \text{kHz}$ . A resonant frequency peak at  $100\ \text{kHz}$ , which is about one third of the value in air was chosen for imaging in liquid. The next step was validating that the measured Young's modulus indeed corresponds to the known value of Young's modulus for PDMS Samples. For this the AFM was switched to force distance spectroscopy mode with the following parameters as shown in Fig. 5.2 below.

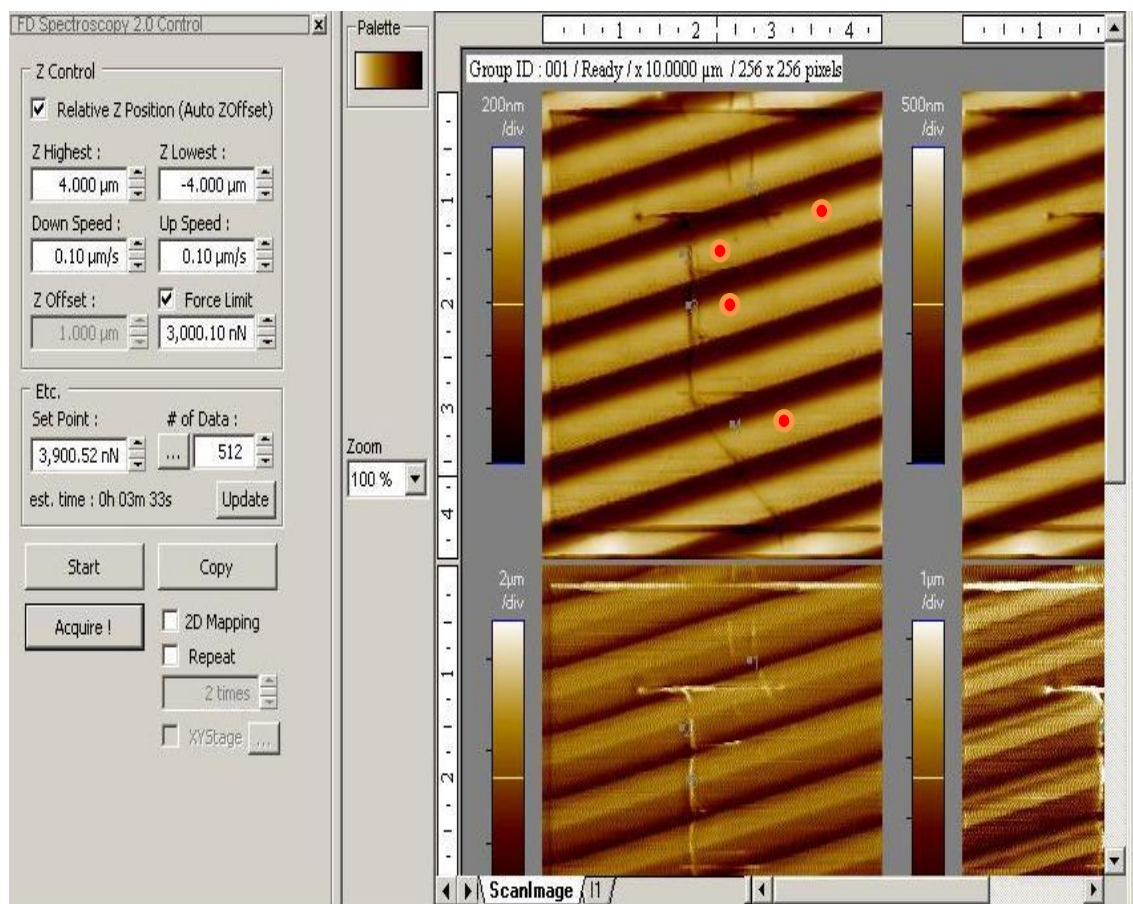


**Fig. 5.2.** Parameters used in the force distance spectroscopy measurements for PDMS samples with red dots showing points which were marked for force distance spectroscopy measurements.

For the measurements, a very high force limit was kept around 4000 nN with a setpoint close to the limit. As the Young's modulus of PDMS is about 10 times higher a force limit 10 times higher was used. As the sample was supposed to be only 1 micrometer high, Z highest and Z lowest as +/- 4 micrometers were fair enough. Finally, the force distance spectroscopy was carried out at 3 points whose results are shown in Fig. 5.3. As the measurements were carried out in liquid medium there were virtually no adhesion effects seen during pull out of the tip from the sample. The force distance spectroscopy graphs of three of the four points shown with white dots in Fig. 5.2 can be seen in Fig.5.3 below.

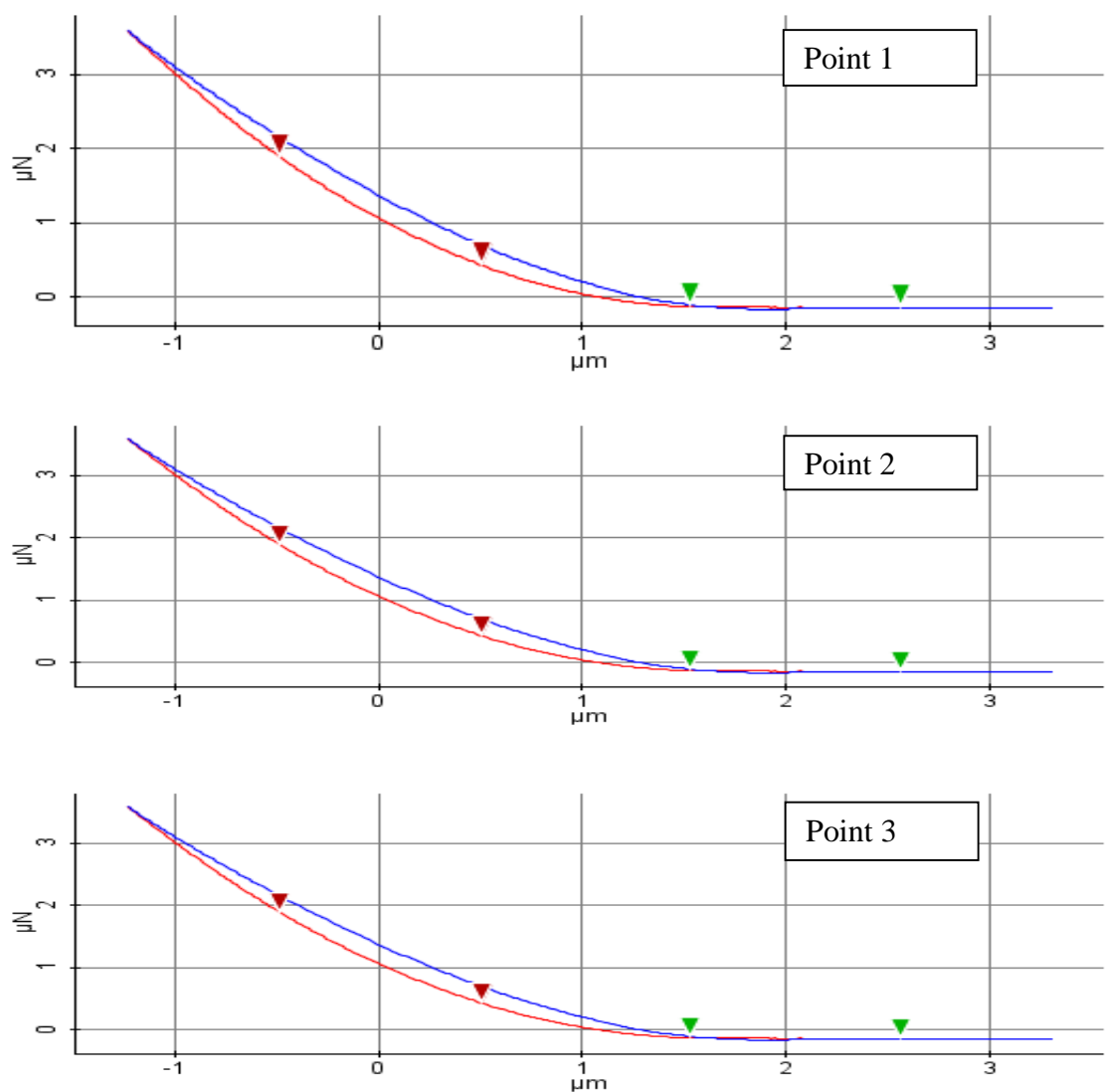


**Fig.5.3. Force distance spectroscopy curves at three arbitrary points on the PDMS samples with vertical axis denoting the AFM Tip and sample interaction force and horizontal axis denoting the distance of approach of the AFM tip to sample .**

To find out the Young's modulus of the sample, the force data and the distance of approach were used from the force distance spectroscopy curves. The same formulas as described in equation 4.1 and 4.2 were used.

In the first curve of Fig 5.3, the force of interaction  $F(h)$  is 310 nN and the distance of approach ( $h$ ) is 2.7  $\mu\text{m}$ . The value of  $R$  used is the radius of the tip, taken from the manufacturer's specification of ACTA cantilevers. It varies from 100 to 300 nm and so a value of 200 nm was considered. Normally, for PDMS samples, a Poisson's ratio of 0.5 is assumed. Further data were obtained at four more points and the results are presented in table 5.1. To validate the results obtained with PDMS all the other samples were also tested and the results of Young's modulus were found to be identical. The average value of Young's modulus was found to be 1.11 MPa for the given samples which had a 10:1 base to curing agent ratio.

**Table 5.1: Young's modulus found by averaging force distance spectroscopy curves of the 1 $\mu\text{m}$  by 3 $\mu\text{m}$  PDMS sample at 8 different points with first three points shown in fig. 5.3.**

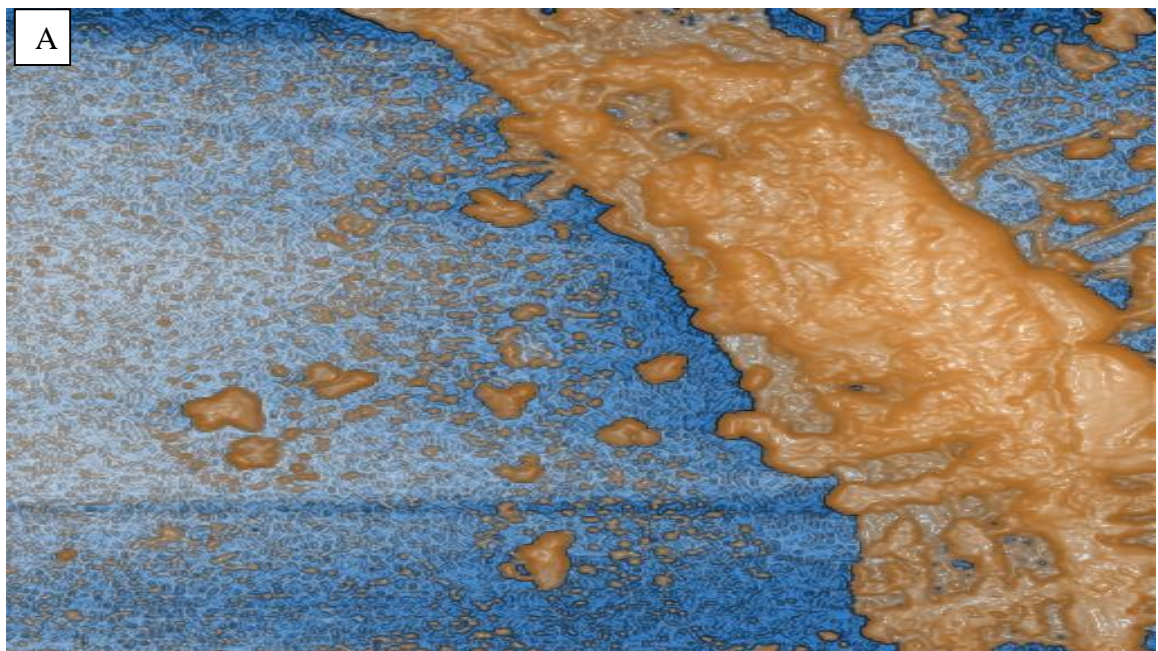
Point	R ( $\mu\text{m}$ )	H ( $\mu\text{m}$ )	F ( $\mu\text{N}$ )	Effective E (MPa)	Actual E (MPa)	Average E (MPa)
1	0.2	2.7	3.1	1.56	1.17	1.11
2	0.2	2.8	3.15	1.50	1.12	
3	0.2	2.9	3.18	1.43	1.07	
4	0.2	2.85	3.13	1.45	1.09	
5	0.2	2.7	3.11	1.56	1.17	
6	0.2	2.8	3.1	1.47	1.10	
7	0.2	2.9	3.11	1.40	1.05	
8	0.2	2.85	3.07	1.42	1.07	

## 5.2 END 2 cells and cardiomyocytes: Imaging and Young's modulus measurements

Three samples of END 2 cell samples and nine samples of fixed dead cardiomyocytes were provided by the Heart Group (BioMediTech, University of Tampere). These samples were successfully imaged in liquid medium containing PBS solution and force distance spectroscopy was also carried out with these samples. Fig.5.4 shows two of the various images obtained with END 2 cells and fixed cardiomyocytes.

Fig. 5.4A shows an enhanced topographical image of an End 2 cell. It is possible to get such enhanced images by using the image enhancing features in XEI, the Image Analysis software. A three dimensional version of the same image is shown in Fig. 5.4B. The three dimensional image shows the XY coordinates which is the scan area and the vertical scale shows the height of the cell. The cardiomyocytes are bigger in size compared to the scan area of the AFM XE 100, so it is difficult to get a prominent image. For example, a single cardiomyocyte can be more than 60 micrometers by 60 micrometers in the X and Y directions respectively.

As the maximum scan area possible with XE 100 AFM is only 45 micrometers by 45 micrometers, it is often difficult to differentiate the surrounding medium from the cardiomyocyte in the topographical image. However, the force distance curves obtained for both the type of cells were quite accurate and corresponded to the expected Young's modulus value found in literature [46]. For imaging the cell samples in liquid, the intermittent mode of imaging was selected. The scan rate was kept low at 0.2 Hz, Z servo gain was 6.5 and the scan size was 40  $\mu\text{m}$  by 40  $\mu\text{m}$  in the XY direction. The cantilever used was the same ACTA cantilever whose resonant frequency in liquid was 100 KHz.



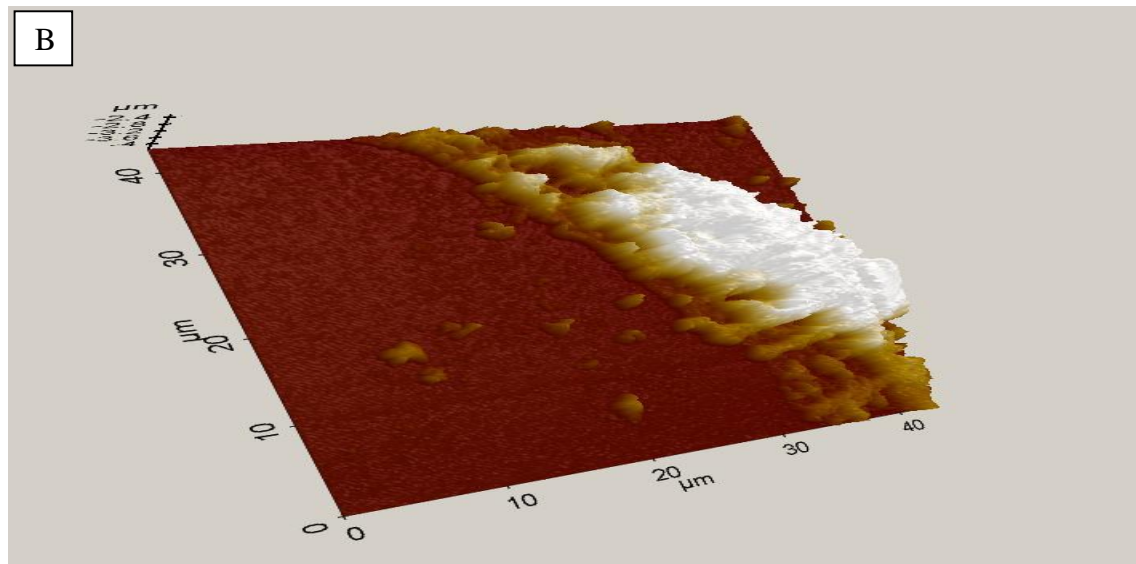


**Fig. 5.4. A) Enhanced Topographical image of a cardiomyocyte. B) 3D view of a cardiomyocyte.**

The images were analyzed with XEI image processing software as in case of PDMS. The heights of END 2 cells and cardiomyocytes were found to be in the range of 300 to 500 nanometers. This can also be understood by taking a look at Fig.5.4B which is the 3D view of the END 2 cell. For imaging the cell samples in liquid, the intermittent mode of imaging was selected. The scan rate was kept low at 0.2 Hz, Z Servo Gain was 6.5 and the scan size was 40  $\mu\text{m}$  by 40  $\mu\text{m}$  in the XY direction. The next step was validating that the measured Young's modulus indeed corresponds to the known value of Young's modulus for End 2 and cardiomyocyte samples. To calculate the Young's modulus, the force distance spectroscopy was again used with the following parameters for both END 2 and cardiomyocyte samples:

Z highest: +4 micrometers

Z lowest: - 4 micrometers

Down Speed: 0.1 micrometer per second

Up Speed: 0.1 micrometer per second

Z offset: 1 micrometer (by default)

Force limit: 1000 nN

Setpoint: 600 nN

A lower force limit of 1000 nN was chosen as these were softer cellular samples compared to PDMS at a setpoint of 600 nN. Also, a softer cantilever should be used for

beating cardiomyocytes, but as there was no chance of damage to fixed cardiomyocytes, the measurements were done with the ACTA cantilever at a lower force limit. Finally, the force distance spectroscopy was carried out at eight points on the topography for both types of cells and one sample curve for each type of sample as shown in Fig. 5.5. As the measurements were carried out in liquid medium with such soft matter as cells so there was virtually no adhesion effects seen during pull out of the tip from the sample.

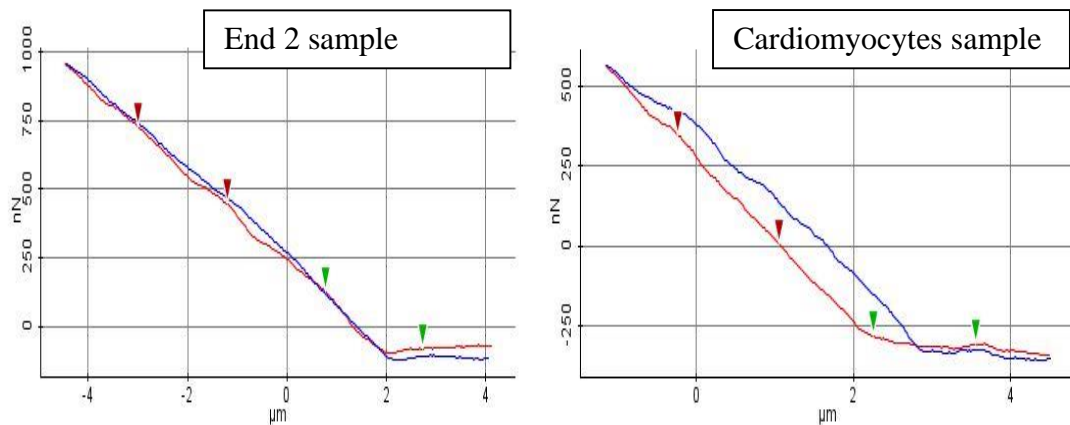


**Fig. 5.5. Force distance curves for fixed End 2 and cardiomyocyte samples respectively.**

With identical force setpoint and force limits for both cardiomyocytes and End 2 cells the maximum force of tip sample interaction was found. It was seen that as the cells are much softer, so the cantilever reaches its maximum interaction force after traversing a much longer distance compared to PDMS. It was found that the END 2 cells were slightly stiffer than the cardiomyocytes even though the difference was not that great. Table 5.2 compiles the stiffness values at 8 different points each of one END 2 sample and one fixed dead cardiomyocyte sample. While the END 2 cells had a stiffness value of about 130 kPa, the Young's modulus for fixed cardiomyocytes was about 104 kPa. As already discussed in section 5.1, to find out the Young's modulus of the sample, the force data and the distance of approach were used from the force distance spectroscopy curves.

A comparison with literature values [9, 10, 45] showed that the Young's modulus of cardiomyocytes is typically in the range of 90 to 110 kPa. So, a value of 104 kPa for Young's modulus of cardiomyocytes was quite within the range.

**Table 5.2: Young's modulus found by averaging force distance spectroscopy curves of the END 2 sample and cardiomyocyte samples with 8 different points for each sample.**

Sample	R( $\mu\text{m}$ )	H ( $\mu\text{m}$ )	F ( $\mu\text{N}$ )	Effective E (MPa)	Actual E (MPa)	Average E (MPa)
End 2 cell	0.1	6.5	0.9	0.171	0.128	0.131
	0.1	6.45	0.9	0.173	0.130	
	0.1	6.5	0.89	0.169	0.127	
	0.1	6.35	0.88	0.173	0.130	
	0.1	6.5	0.92	0.175	0.131	
	0.1	6.45	0.91	0.175	0.131	
	0.1	6.5	0.92	0.175	0.131	
	0.1	6.4	0.92	0.179	0.134	
Fixed cardiomyocyte	0.1	5	0.52	0.147	0.110	0.104
	0.1	5.1	0.51	0.140	0.105	
	0.1	5.4	0.52	0.131	0.098	
	0.1	5.5	0.53	0.129	0.097	
	0.1	5.1	0.51	0.140	0.105	
	0.1	5.1	0.52	0.142	0.107	
	0.1	5.1	0.52	0.142	0.107	
	0.1	5.25	0.52	0.136	0.102	

### 5.3 Beating force measurements in heart cells.

A unique and novel method was adopted for measuring the beating forces of the stem cell derived cardiomyocytes and will be discussed in details in this section. For making the measurements, the liquid cell was set up as normal and then covered with the closed liquid cell cover. Finally, a cover glass was put on top of it to prevent the evaporation of Elliott solution used for culturing the cardiomyocytes at 37 degree Centigrade. The arrangement is shown in the figure 5.6 below.

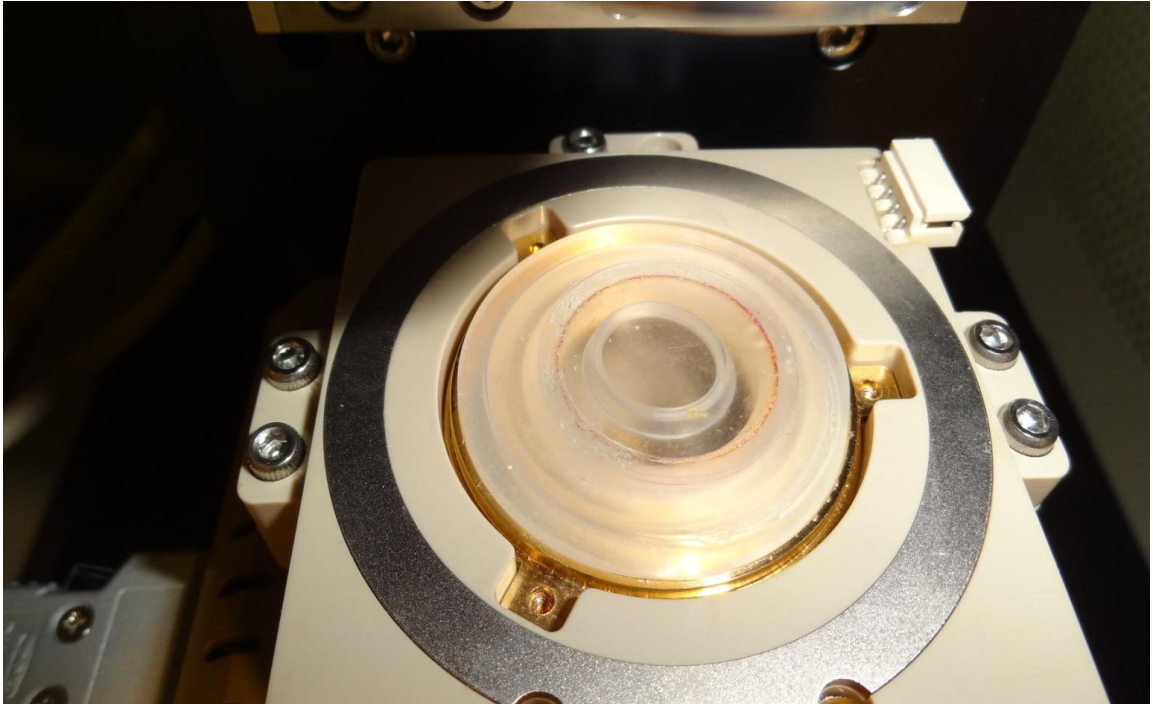


**Fig. 5.6. Arrangement of liquid cell with a closed cover and a cover glass slide to maintain the temperature inside the liquid cell at 37 degree C and prevent the Elliott solution to evaporate.**

The AFM probe holder for the liquid cell was also covered with another closed liquid cell cover. The intention was to prevent the evaporation of Elliott solution at 37 degree Centigrade during the time the AFM head was lowered onto the liquid cell. Normally, the process of finding the cantilever for the AFM head and then focusing the laser on top of the tip of the cantilever takes about a few minutes. But as the liquid cell was covered there was no chance of the Elliott solution evaporating anymore during these few minutes. The cardiomyocytes were transported from the University of Tampere tightly packed in a travel incubator. The idea was to expose the cells to the room temperature for the minimum time possible. The Elliott solution heated up to 37 degree Centigrade was stored momentarily in pipette and the cover slide containing the cardiomyocyte was lowered into the liquid cell. The arrangement of the AFM head for making temperature sensitive measurements is shown in Fig. 5.7.

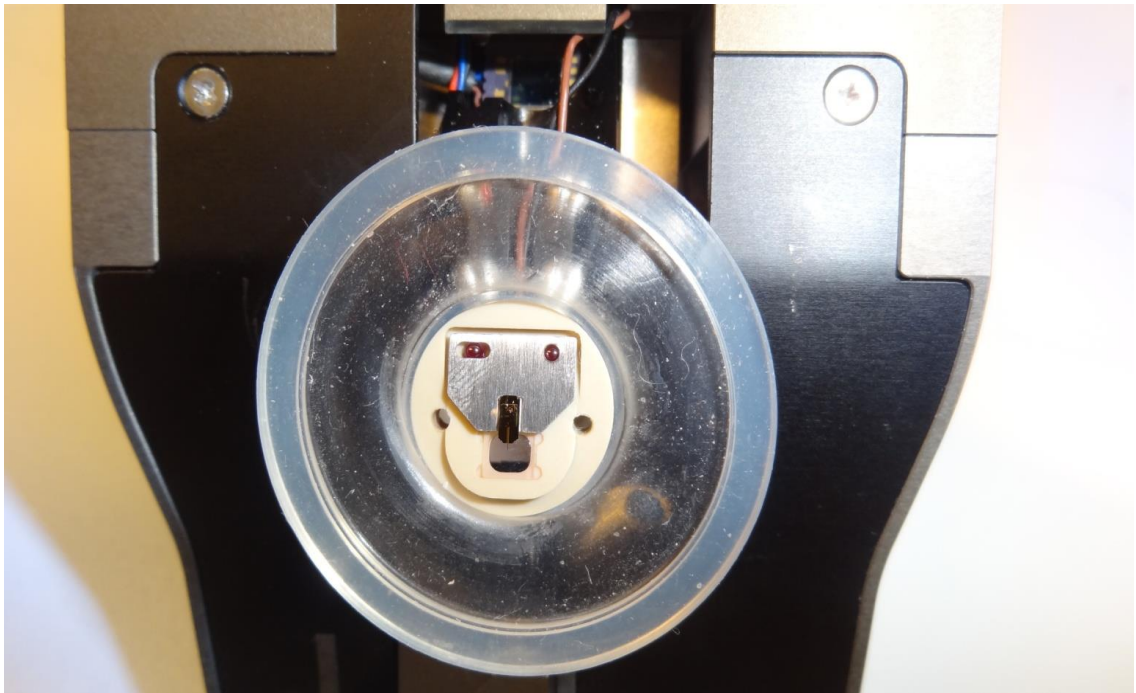
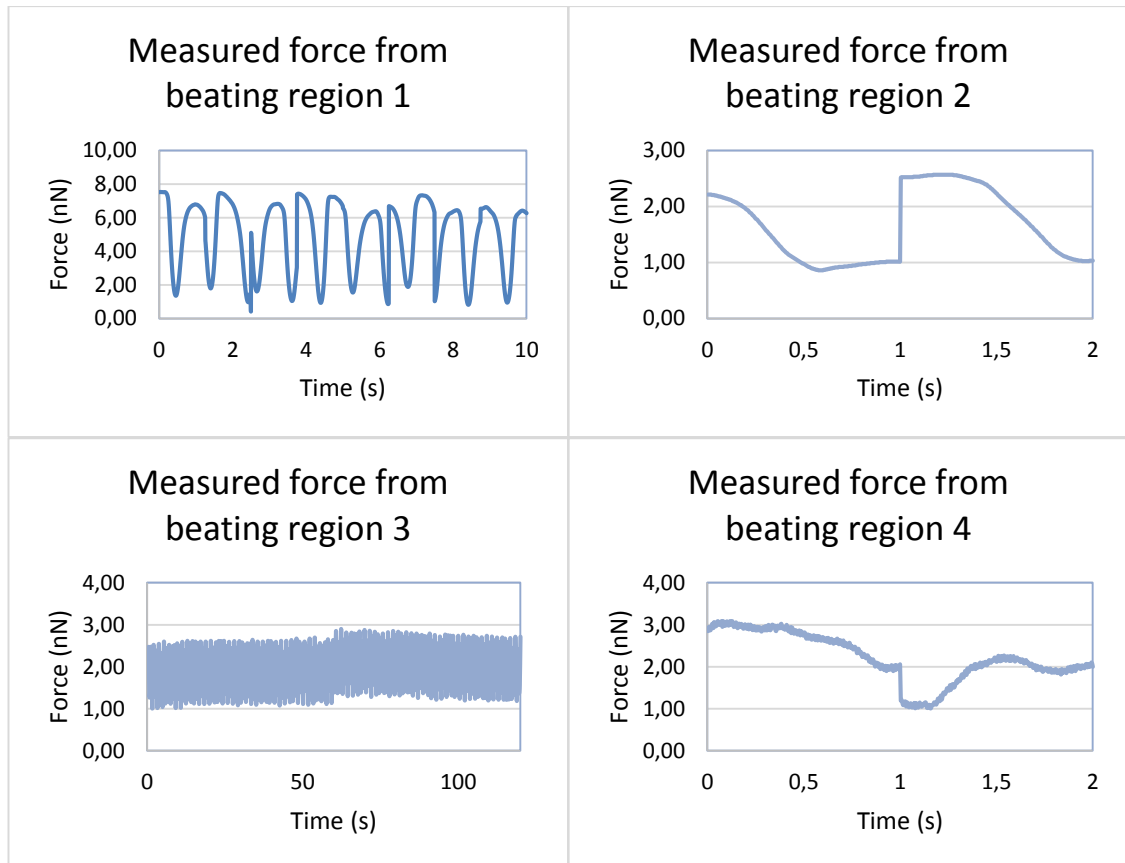


**Fig. 5.7. AFM head arrangement which that the cantilever is housed in a closed liquid cell as the head is lowered onto the sample.**

The next step was lowering the cantilever tip onto the beating cardiomyocyte samples. The scan size of the AFM head was set to zero so that the tip was stationary as it was lowered onto the sample. This ensured that there was minimum interference from the AFM and what was recorded was exactly the displacement signals coming from the beating cardiomyocytes. A periodic beating signal coming from the samples was observed with maximum displacements ranging from 40 to 120 nanometers at different regions of the sample. The difference in beating forces was ascertained to the fact that some of the cells were isolated while some of them were in beating clusters. Also some cells were about to die which meant that they were beating with lesser forces compared with the normal healthy cells. A sample topography curve with the stationary tip obtained from the data acquisition software XEP is shown in fig. 5.8. The obtained graph is shown as force of the beating cardiomyocytes versus time elapsed.



+

**Fig. 5.8. Beating force of the cardiomyocytes acquired from XEP software with the AFM tip stationary at four regions on the sample at four different time intervals showing the displacement of stem cell derived beating cardiomyocytes multiplied with the spring constant.**

Measurements over the beating sample were made at several regions and with a Mikro-masch HQ 17 series cantilever of spring constant 0.06 N/m, whose specifications are mentioned in section 4.3. The beating forces could be obtained by multiplying the beating displacements of the nanoscale tip of the AFM (interacting with the beating cardiomyocyte) directly with the spring constant of the AFM. The frequency of beating of the cardiomyocytes can be calculated by measuring the beat to beat separation or by measuring the number of peaks in a sample measurement of a sufficiently long time like 10 seconds or more. The table 5.3 shows the beating displacements and corresponding beating forces at different regions of the sample containing beating cardiomyocytes. While regions 1, 2, 3 and 4 are the same in fig. 5.8 as in table 5.3, the region 3 was sampled over a long interval of 120 seconds and had to be shown in smaller intervals (of 20seconds each) to have a closer look at region 3. This is shown in Fig. 5.9 where region 3 of measurement is divided into six sub regions to verify the consistency of the data shown in fig. 5.8. This was also necessary as the data had to be collected both over different regions of the sample as well as at sufficient time intervals. Thus, Fig. 5.9

shows the data collected over a time period of 120 seconds over region 3 divided into 6 smaller regions of 20 seconds each. The results of Fig. 5.8 and 5.9 were compiled into table 5.3 as shown below.

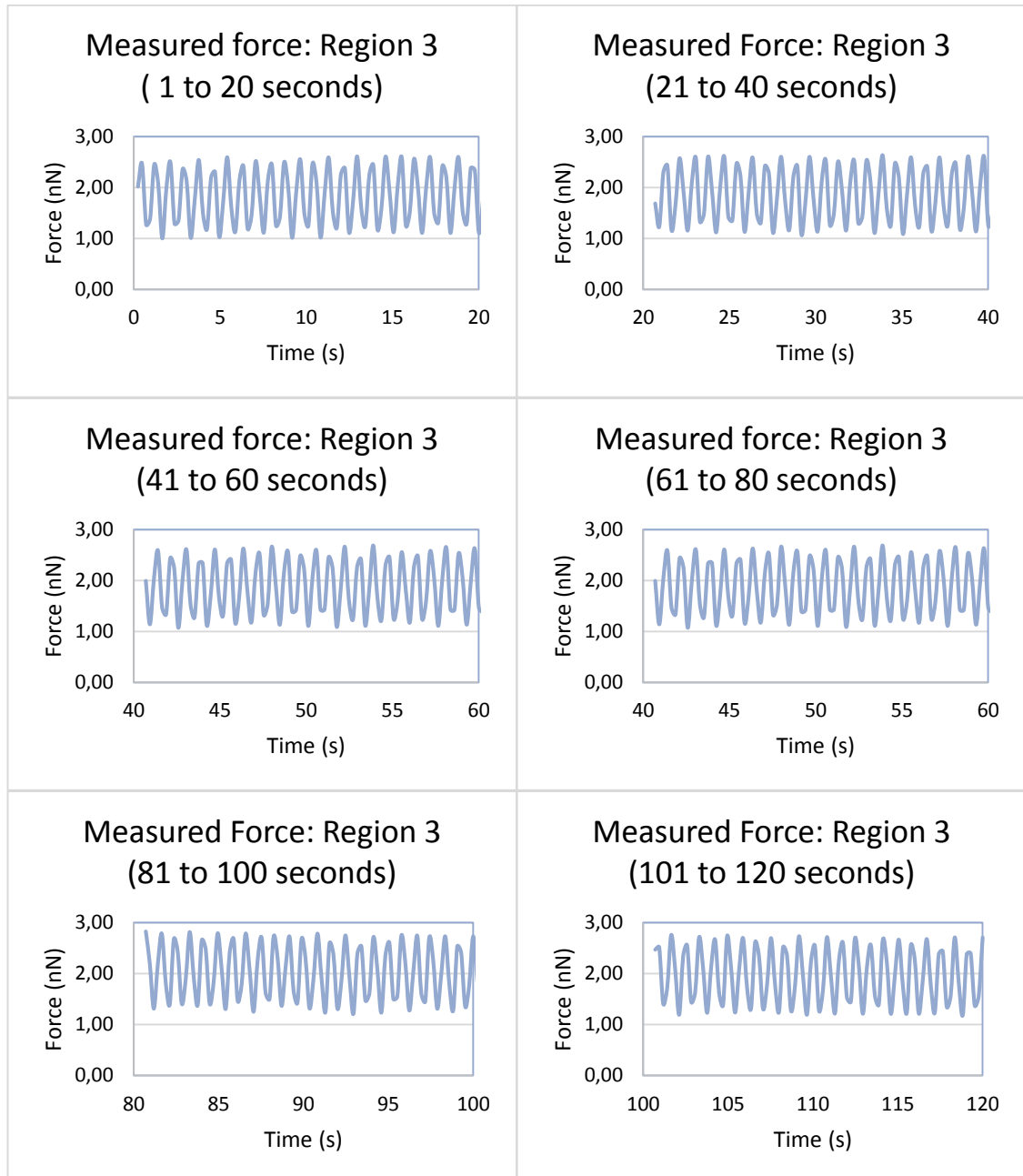


**Fig. 5.9. Measured Beating force of the cardiomyocytes acquired from XEP software with the AFM tip stationary at Region 3 on the sample at same time intervals of 20 seconds each showing the displacement of stem cell derived beating cardiomyocytes multiplied with the spring constant.**

**Table 5.3. Beating forces of cardiomyocytes at four different regions of measurement.**

Region of measurement	Average beating amplitude( $\mu\text{m}$ )	Average standard deviation( $\mu\text{m}$ )	Average beating force (nN)	Number of peaks	Average beating frequency (per min)	Length of sampling period (seconds)
Region 1	0.116	0.0362	6.93	10	60	10
Region 2	0.0424	0.0105	2.54	2	60	2
Region 4	0.0474	0.0096	2.84	2	60	2
Region 3 ( 1 to 20 s)	0.0429	0.0091	2.57	23	69	20
Region 3 (21 to 40 s)	0.0431	0.0089	2.58	23	69	20
Region 3 (41 to 60s)	0.0437	0.0091	2.62	22	66	20
Region 3 (61 to 80 s)	0.0451	0.0089	2.79	23	66	20
Region 3 (81 to 100 s)	0.0449	0.0090	2.69	24	72	20
Region 3 (101 to 120 s)	0.0442	0.0090	2.65	21	63	20

Regions 1 to 4 in table 5.3 show the beating forces over 4 different regions in the sample while Region 3 is divided into 6 sections as the data collected was over a time inter-

val of 120 seconds. The beating forces were measured over various regions of the sample and some data has been reported in Table 5.3. It comprises four beating regions. To validate the novelty of the method it was necessary to test it both at different regions, at different time intervals as well as over sufficient duration of time and this is achieved in the measurements as shown in Table 5.3. The maximum beating forces were reported in the range of 2.5 nN to 7 nN. Region 1 has greater forces compared to remaining regions as possibly it was a cluster of cells with several beating cells leading to greater force exertion. The maximum beating force was the highest deviation from the zero value and the maximum beating force was calculated by multiplying the maximum force with the spring constant. The measurement data was processed according to the protocol mentioned in section 4.3. The actual maximum beating force is 1 nN higher than what was recorded directly by the AFM as the contact force of the cantilever to the sample needs to be added.

## 6. CONCLUSION AND FUTURE WORK

The main objective of this thesis was to provide a solution to a long awaited requirement of the Heart Group at BioMediTech, University of Tampere, which was to measure beating forces of heart cells. A meaningful contribution has been made in measuring the beating force of stem cell derived cardiomyocytes and more importantly a protocol has been established for making such measurements in future with the AFM. The thesis started with a literature review of possible methods for force measurements of cardiomyocytes. The aim of the literature review was to bring together at one place all the methods and inventions that are already existing for the measurement of contractile force of cardiomyocytes. A careful analysis of the methods resulted in choosing the AFM as the most suitable measurement method. The reasons were the widest range of force measurements possible with one device and the accuracy of the device, as it has been discussed earlier.

The measurements conducted with the AFM were direct recordings from the beating cardiomyocytes seen in terms of displacement of the cantilever probing it. This makes it a highly accurate method with no complex mathematical formulations needed to derive the actual force as in most of the other methods discussed in section 2 of this thesis. This kind of work was quite unique compared to similar efforts that has been done in the past as in this novel approach the AFM tip was actually stationary over the dynamic medium. Previously, the z axis of the piezo actuator of AFM had to be synchronized with the beating of the cardiomyocytes which was in itself quite complicated and this also created fluidic disturbances. A description of the AFM parameters that were used and the detailed protocol that was followed for making such measurements is presented in this thesis for researchers to carry out similar measurements in future.

The Heart Group is working on different genetic heart diseases. It is expected that the diseased heart cells will have different rhythm of beating as well as different forces exerted than normal heart cells. By devising a highly accurate method to measure the beating forces of heart cells as well as the beating frequency, it will be possible to differentiate the normal and diseased heart cells. This might have tremendous implications in future diagnostics of genetic heart diseases.

A potential enhancement to this method can be automatization of the whole process so that a biologist does not have to spend hours in the laboratory just trying to fine tune the parameters of the AFM. Indeed, some new AFMs have come up (for example, Park Systems AFM XE Bio) which are fully automatic. In spite of its advantages, there are some disadvantages related to the XE 100 like the long time required in understanding each and every function of the parameters used in imaging and force distance spectroscopy. Someone working without a full understanding of the device might break the cantilever tip, cause damage to the device and the user can also end up harming himself. This is something which does not make it really friendly to use for the biologists.

To study diseases related to the human heart, it is necessary to know the contractile state, mechanical properties and the mechanotransduction process, all of which can be traced down to the single cell level. There is a need for the development of new measurement techniques which will be able to give answers to questions that constantly keep coming up as we go closer and closer to developing the first human spare heart which is functioning perfectly. In future, one of the challenges will be extending measurement techniques to subcellular level. Current techniques allow the measurement or detection of forces only up to the piconewton range, but for subcellular level studies we might need to measure forces at subcellular level. That can allow force measurements in the femtonewton range even though thermal effects come into play at that stage.

This protocol can prove useful for studying heart diseases as the contractile state and beating forces have been suitably measured using this method. The measured values can be used to differentiate the healthy cardiomyocytes from the diseased ones based on the beating forces exerted and the frequency of heartbeats. It should be noted that what we are actually measuring here is the displacement of the cantilever touching the beating cardiomyocyte. However, as the cantilever is in direct contact with a cardiomyocyte, its displacement can be correctly attributed as the displacement of the cardiomyocyte. A small force is applied on the cardiomyocyte to hold the cantilever on to its surface and to establish contact but then this force is very small and is known too. So, this means that displacement we are getting should be converted to beating force and then the force of contact added to get the true beating force.

There were several challenges faced during the course of the thesis. Firstly, imaging a soft sample in liquid with the AFM XE 100 is quite challenging and needs hours of tuning of the parameters to come up with some concrete results. Secondly, a lot of time is needed to familiarize with the hundreds of features available with the AFM software. Thirdly, a lot of experimentation had to be done to find to select the most suitable cantilever for extracting meaningful information like Young's modulus and cell stiffness from the observed force distance curves. Last but not the least, the cells had to be transported from University of Tampere to Tampere University of Technology and extreme carefulness was needed to ascertain that the cells survived in this passage of time. A travel incubator was used to maintain the temperature of the cells at 37 degrees C. An even bigger challenge was making the cells survive when it was transferred from the travel incubator to the AFM liquid cell.

A good way to improve this process will be making the AFM based measurements inside the cell culturing vessel directly and at the cell culturing location, when no transporting of the cells is needed. Another method can be designing a travel incubator which can fit directly under the AFM. It is also possible to grow a cell sample directly on the universal liquid cell and then transport the whole liquid cell under the AFM, even though this might prove a bit expensive in larger scale. But then the universal liquid cell needs to be maintained at 37 degree Centigrade. If not exposed to a temperature below 37 degree Centigrade for too long, the cells survive for about 2 hours which is good enough time for making the measurements.

To conclude, a novel method for measuring the beating forces of stem cell derived cardiomyocytes was discovered. The mechanobiological properties of pluripotent stem cell-derived cardiomyocytes were measured which included frequency of beats, duration, cellular elasticity and a common set of parameters were identified for each of the imaging modes and force distance spectroscopy for making such measurements in future.

## REFERENCES

- [1] Okita, K., Ichisaka, T., & Yamanaka, S. (2007). Generation of germline-competent induced pluripotent stem cells. *Nature*, *448*, 313–317. doi:10.1038/nature05934.
- [2] Takahashi, K., Tanabe, K., Ohnuki, M., Narita, M., Ichisaka, T., Tomoda, K., & Yamanaka, S. (2007). Induction of Pluripotent Stem Cells from Adult Human Fibroblasts by Defined Factors. *Cell*, *131*, 861–872. doi:10.1016/j.cell.2007.11.019.
- [3] Takahashi, K., & Yamanaka, S. (2006). Induction of Pluripotent Stem Cells from Mouse Embryonic and Adult Fibroblast Cultures by Defined Factors. *Cell*, *126*, 663–676. doi:10.1016/j.cell.2006.07.024.
- [4] Park, I.-H., Arora, N., Huo, H., Maherali, N., Ahfeldt, T., Shimamura, A., Daley, G. Q. (2008). Disease-specific induced pluripotent stem cells. *Cell*, *134*, 877–886. doi:10.1016/j.cell.2008.07.041.
- [5] Sun, N., Yazawa, M., Liu, J., Han, L., Sanchez-Freire, V., Abilez, O. J., Wu, J. C. (2012). Patient-specific induced pluripotent stem cells as a model for familial dilated cardiomyopathy. *Science Translational Medicine*, *4*, 130ra47. doi:10.1126/scitranslmed.3003552.
- [6] Ebert, A. D., Liang, P., & Wu, J. C. (2012). Induced Pluripotent Stem Cells as a Disease Modeling and Drug Screening Platform. *Journal of Cardiovascular Pharmacology*. doi:10.1097/FJC.0b013e318247f642.
- [7] Cogollo, J. F. S., Tedesco, M., Martinoia, S., & Raiteri, R. (2011). A new integrated system combining atomic force microscopy and micro-electrode array for measuring the mechanical properties of living cardiac myocytes. *Biomedical Microdevices*, *13*, 613–621. doi:10.1007/s10544-011-9531-9.
- [8] Park Systems AFM XE 100 User Manual [WWW]. [Accessed on 14.4.2014]. Available at: <http://research.fit.edu/nhc/documents/XE100UserManual.pdf>.
- [9] Mathur, A. B., Collinworth, A. M., Reichert, W. M., Kraus, W. E., & Truskey, G. A. (2001). Endothelial, cardiac muscle and skeletal muscle exhibit different viscous and elastic properties as determined by atomic force microscopy. *Journal of Biomechanics*, *34*, 1545–1553. doi:10.1016/S0021-9290(01)00149-X.
- [10] Addae-Mensah, K. A., & Wikswo, J. P. (2008). Measurement techniques for cellular biomechanics in vitro. *Experimental Biology and Medicine (Maywood, N.J.)*, *233*, 792–809. doi:10.3181/0710-MR-278.
- [11] Yin, S., Zhang, X., Zhan, C., Wu, J., Xu, J., & Cheung, J. (2005). Measuring single cardiac myocyte contractile force via moving a magnetic bead. *Biophysical Journal*, *88*, 1489–1495. doi:10.1529/biophysj.104.048157

- [12] Chien, S., Sung, K. L., Skalak, R., Usami, S., & Tözeren, A. (1978). Theoretical and experimental studies on viscoelastic properties of erythrocyte membrane. *Biophysical Journal*, *24*, 463–487. doi:10.1016/0026-0495(78)90289-5.
- [13] Schmid-Schonbein, G. W., Sung, K.-L. P. L. K., Tozeren, H., Skalak, R., Chien, S., Schmid-Schönbein, G. W., & Shalak, R. (1981). Passive mechanical properties of human leukocytes. *Biophysical Journal*, *36*, 243–256. doi:10.1016/S00063495(81)84726-1.
- [14] Chu, Y.-S., Thomas, W. A., Eder, O., Pincet, F., Perez, E., Thiery, J. P., & Dufour, S. (2004). Force measurements in E-cadherin-mediated cell doublets reveal rapid adhesion strengthened by actin cytoskeleton remodeling through Rac and Cdc42. *The Journal of Cell Biology*, *167*, 1183–1194. doi:10.1083/jcb.200403043.
- [15] Linder, P., Trzewik, J., Ruffer, M., Artmann, G. M., Digel, I., Kurz, R., & Temiz Artmann, A. (2010). Contractile tension and beating rates of self-exciting monolayers and 3D-tissue constructs of neonatal rat cardiomyocytes. *Medical and Biological Engineering and Computing*, *48*, 59–65. doi:10.1007/s11517-009-0552-y.
- [16] Trzewik, J., Ates, M., & Artmann, G. M. (2002). A novel method to quantify mechanical tension in cell monolayers. *Biomedizinische Technik. Biomedical Engineering*, *47 Suppl 1 Pt 1*, 379–381. doi:10.1515/bmte.2002.47.s1a.379.
- [17] Trzewik, J., Artmann-Temiz, A., Linder, P. T., Demirci, T., Digel, I., & Artmann, G. M. (2004). Evaluation of lateral mechanical tension in thin-film tissue constructs. *Annals of Biomedical Engineering*, *32*, 1243–1251. doi:10.1114/B:ABME.0000039358.71180.9a.
- [18] Iribe, G., Helmes, M., & Kohl, P. (2007). Force-length relations in isolated intact cardiomyocytes subjected to dynamic changes in mechanical load. *American Journal of Physiology. Heart and Circulatory Physiology*, *292*, H1487–H1497. doi:10.1152/ajpheart.00909.2006.
- [19] Palmer, R. E., Brady, A. J., & Roos, K. P. (1996). Mechanical measurements from isolated cardiac myocytes using a pipette attachment system. *The American Journal of Physiology*, *270*, C697–C704.
- [20] Sugiura, S., Nishimura, S., Yasuda, S., Hosoya, Y., & Katoh, K. (2006). Carbon fiber technique for the investigation of single-cell mechanics in intact cardiac myocytes. *Nature Protocols*, *1*, 1453–1457. doi:10.1038/nprot.2006.241.
- [21] Iribe, G., Ward, C. W., Camelliti, P., Bollensdorff, C., Mason, F., Burton, R. A. B., & Kohl, P. (2009). Axial stretch of rat single ventricular cardiomyocytes causes an acute and transient increase in Ca<sup>2+</sup> spark rate. *Circulation Research*, *104*, 787–795. doi:10.1161/CIRCRESAHA.108.193334.
- [22] Shimizu, K., Hoshino, T., Akiyama, Y., Iwabuchi, K., Yamato, M., Okano, T., & Morishima, K. (2010). Multi-scale reconstruction and performance of insect mus-

- cle powered bioactuator from tissue to cell sheet. In *2010 3rd IEEE RAS and EMBS International Conference on Biomedical Robotics and Biomechatronics, BioRob 2010* (pp. 425–430). doi:10.1109/BIOROB.2010.5626762
- [23] Shimizu, K., Hoshino, T., Akiyama, Y., Iwabuchi, K., Yamato, M., Okano, T., & Morishima, K. (2010). Multi-scale reconstruction and performance of insect muscle powered bioactuator from tissue to cell sheet. In *2010 3rd IEEE RAS and EMBS International Conference on Biomedical Robotics and Biomechatronics, BioRob 2010* (pp. 425–430). doi:10.1109/BIOROB.2010.5626762.
- [24] Boudou, T., Legant, W. R., Mu, A., Borochn, M. A., Thavandiran, N., Radisic, M., Chen, C. S. (2012). A Microfabricated Platform to Measure and Manipulate the Mechanics of Engineered Cardiac Microtissues. *Tissue Engineering Part A*. doi:10.1089/ten.tea.2011.0341.
- [25] Bajaj, P., Tang, X., Saif, T. A., & Bashir, R. (2010). Stiffness of the substrate influences the phenotype of embryonic chicken cardiac myocytes. *Journal of Biomedical Materials Research - Part A*, 95, 1261–1269. doi:10.1002/jbm.a.32951.
- [26] Orfanidou, T., Papaefthimiou, C., Antonopoulou, E., Leonardos, I., & Theophilidis, G. (2013). The force of the spontaneously contracting zebrafish heart, in the assessment of cardiovascular toxicity: Application on adriamycin. *Toxicology in Vitro*, 27, 1440–1444. doi:10.1016/j.tiv.2013.03.004.
- [27] Xi, J., Khalil, M., Shishechian, N., Hannes, T., Pfannkuche, K., Liang, H., Pillekamp, F. (2010). Comparison of contractile behavior of native murine ventricular tissue and cardiomyocytes derived from embryonic or induced pluripotent stem cells. *The FASEB Journal : Official Publication of the Federation of American Societies for Experimental Biology*, 24, 2739–2751. doi:10.1096/fj.09-145177.
- [28] Lee, J., Leonard, M., Oliver, T., Ishihara, A., & Jacobson, K. (1994). Traction forces generated by locomoting keratocytes. *The Journal of Cell Biology*, 127, 1957–1964. doi:10.1083/jcb.127.6.1957.
- [29] Lee, J., Leonard, M., Oliver, T., Ishihara, A., & Jacobson, K. (1994). Traction forces generated by locomoting keratocytes. *The Journal of Cell Biology*, 127, 1957–1964. doi:10.1083/jcb.127.6.1957.
- [30] Balaban, N. Q., Schwarz, U. S., Rivelino, D., Goichberg, P., Tzur, G., Sabanay, I., Geiger, B. (2001). Force and focal adhesion assembly: a close relationship studied using elastic micropatterned substrates. *Nature Cell Biology*, 3, 466–472. doi:10.1038/35074532.
- [31] Dembo, M., & Wang, Y. L. (1999). Stresses at the cell-to-substrate interface during locomotion of fibroblasts. *Biophysical Journal*, 76, 2307–2316. doi:10.1016/S0006-3495(99)77386-8.
- [32] Hansen, A., Eder, A., Bönstrup, M., Flato, M., Mewe, M., Schaaf, S., Eschenhagen, T. (2010). Development of a drug screening platform based on engineered

- heart tissue. *Circulation Research*, 107, 35–44. doi:10.1161/CIRCRESAHA.109.211458.
- [33] Du Roure, O., Dequidt, C., Richert, A., Austin, R. H., Buguin, A., Chavrier, P., Ladoux, B. (2004). Microfabricated arrays of elastomeric posts to study cellular mechanics. *Proceedings of SPIE*, 5345, 26–34. doi:10.1117/12.530688.
- [34] Hazeltine, L. B., Simmons, C. S., Salick, M. R., Lian, X., Badur, M. G., Han, W., ... Palecek, S. P. (2012). Effects of substrate mechanics on contractility of cardiomyocytes generated from human pluripotent stem cells. *International Journal of Cell Biology*. doi:10.1155/2012/508294.
- [35] Mijailovich, S. M., Kojic, M., Zivkovic, M., Fabry, B., & Fredberg, J. J. (2002). A finite element model of cell deformation during magnetic bead twisting. *Journal of Applied Physiology (Bethesda, Md. : 1985)*, 93, 1429–1436. doi:10.1152/jappphysiol.00255.2002.
- [36] Krueger, J. W., Forletti, D., & Wittenberg, B. A. (1980). Uniform sarcomere shortening behavior in isolated cardiac muscle cells. *The Journal of General Physiology*, 76, 587–607. doi:10.1085/jgp.76.5.587.
- [37] Niggli, E. (1988). A laser diffraction system with improved sensitivity for long-time measurements of sarcomere dynamics in isolated cardiac myocytes. *Pflügers Archiv European Journal of Physiology*, 411, 462–468. doi:10.1007/BF00587728.
- [38] Ivester, C. T., Kent, R. L., Tagawa, H., Tsutsui, H., Imamura, T., Cooper, G., & McDermott, P. J. (1993). Electrically stimulated contraction accelerates protein synthesis rates in adult feline cardiocytes. *The American Journal of Physiology*, 265, H666–H674.
- [39] Dao, M., Lim, C. T., & Suresh, S. (2003). Mechanics of the human red blood cell deformed by optical tweezers. *Journal of the Mechanics and Physics of Solids*. doi:10.1016/j.jmps.2003.09.019.
- [40] Hénon, S., Lenormand, G., Richert, A., & Gallet, F. (1999). A New Determination of the Shear Modulus of the Human Erythrocyte Membrane Using Optical Tweezers. *Biophysical Journal*. doi:10.1016/S0006-3495(99)77279-6.
- [41] Yang, S., & Saif, T. (2005). Micromachined force sensors for the study of cell mechanics. *Review of Scientific Instruments*, 76. doi:10.1063/1.1863792.
- [42] Serrell, D. B., Law, J., Slifka, A. J., Mahajan, R. L., & Finch, D. S. (2008). A uniaxial bioMEMS device for imaging single cell response during quantitative force-displacement measurements. *Biomedical Microdevices*, 10, 883–889. doi:10.1007/s10544-008-9202-7.
- [43] Mummery, C. L., van Achterberg, T. A., van den Eijnden-van Raaij, A. J., van Haaster, L., Willemse, A., de Laat, S. W., & Piersma, A. H. (1991). Visceral-endoderm-like cell lines induce differentiation of murine P19 embryonal carcino-

ma cells. *Differentiation; Research in Biological Diversity*, 46, 51–60. doi:10.1111/j.1432-0436.1991.tb00865.x.

- [44] Mummery, C., Ward-van Oostwaard, D., Doevendans, P., Spijker, R., van den Brink, S., Hassink, R., Tertoolen, L. (2003). Differentiation of human embryonic stem cells to cardiomyocytes: role of coculture with visceral endoderm-like cells. *Circulation*, 107, 2733–2740. doi:10.1161/01.CIR.0000068356.38592.68
- [45] Kuznetsova, T. G., Starodubtseva, M. N., Yegorenkov, N. I., Chizhik, S. A., & Zhdanov, R. I. (2007). Atomic force microscopy probing of cell elasticity. *Micron*, 38, 824–833. doi:10.1016/j.micron.2007.06.011.
- [46] Mahaffy, R. E., Park, S., Gerde, E., Käs, J., & Shih, C. K. (2004). Quantitative Analysis of the Viscoelastic Properties of Thin Regions of Fibroblasts Using Atomic Force Microscopy. *Biophys. J.*, 86, 1777–1793. doi:10.1016/S0006-3495(04)74245-9

## APPENDIX

### A. AFM XE 100 Software

The Park systems AFM XE 100 package comes with three very important software, the camera software XEC, the data acquisition software XEP and the image processing software XEI. The positioning of the tip, the control of the AFM and the processing of the obtained images and results is done by means of these three software. Hence this chapter is devoted to a more thorough understanding of the three software and the parameters that are used during imaging and force measurements.

#### A.1. Camera software XEC

XEC is the Park AFM XE 100 camera software which helps to see the optical microscope image taken by the CCD camera. Also, it helps to see the cantilever approach the sample surface and helps to see the sample surface as well. It helps to find out the interesting area to image on the sample as it gives a good view of the sample surface. It has some features too like grabbing a snapshot of the sample surface and placing a crosshair which helps to locate the cantilever as shown below in Fig A.1.

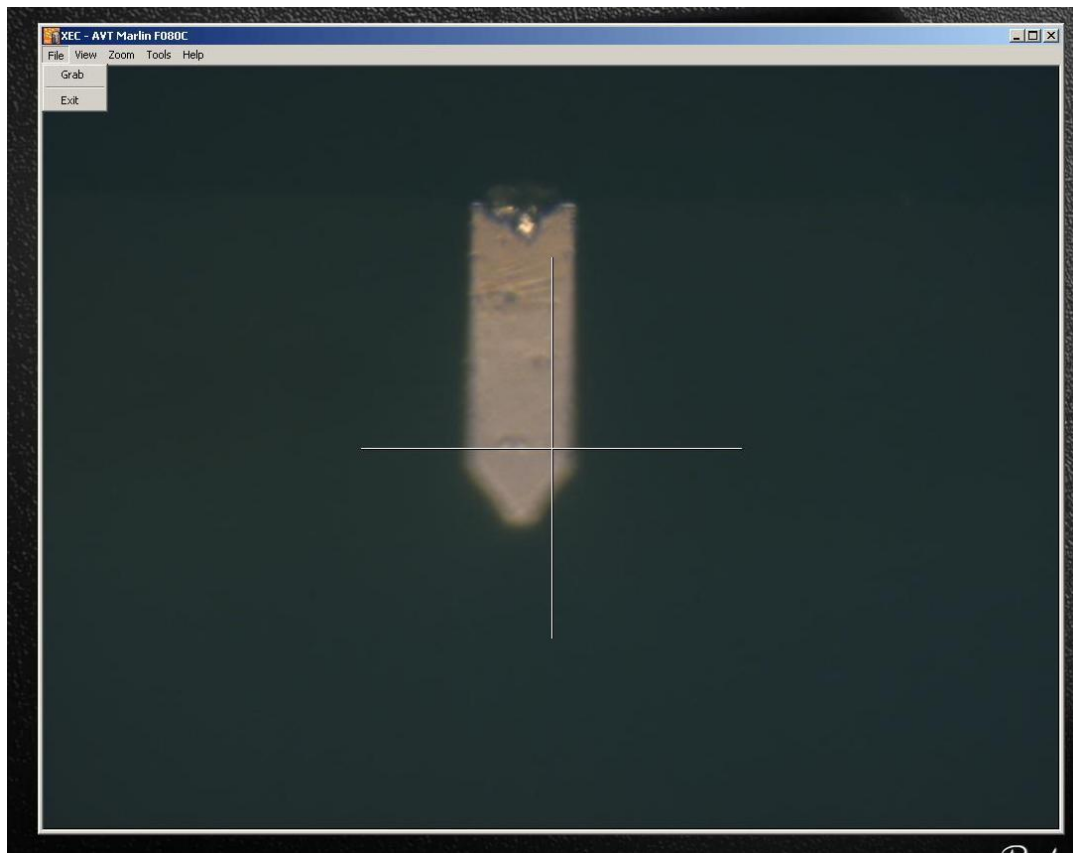


**Fig.A.1** A view of the XEC software with the crossbar and a view of the cantilever.

The software also allows to zoom to the surface and this gives an additional camera zoom in addition to the optical microscope 10 X zoom. It also helps to find out the laser spot on the cantilever before the Z stage is lowered onto the sample.

## A.2. Data Acquisition Software XEP

The Data acquisition software XEP is responsible for operating and controlling the Park Systems AFM XE 100. It has a huge number of features but here the discussion is restricted to the features most necessary for imaging and force distance spectroscopy measurements. The XEP software user interface is divided into several windows as shown below in Fig.A.2.

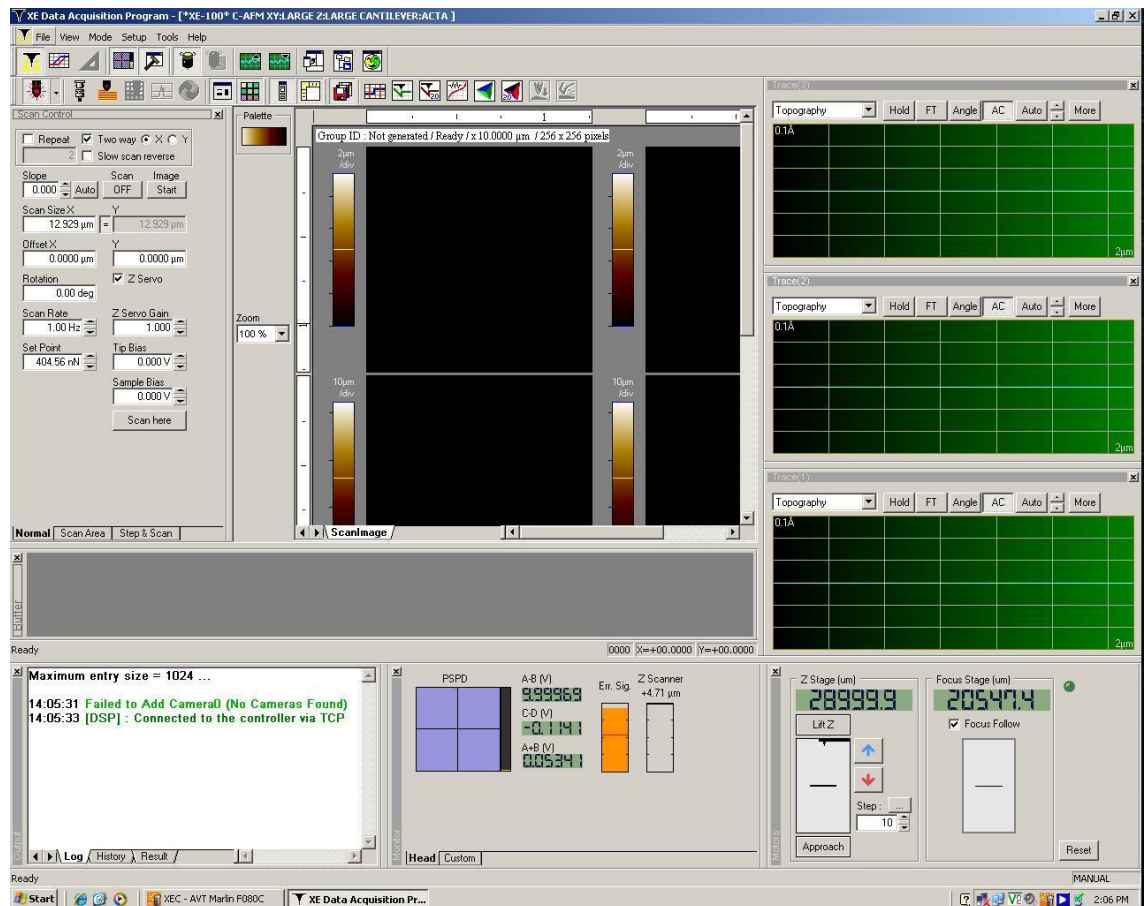


**Fig.A.2 Park Systems AFM XE100 XEP Data Acquisition Software User Interface.**

The different windows on display above are described one by one below along with a short description of the FD Spectroscopy Mode and nano indentation mode:

a) Scan Control window - This is used for setting up a scan and taking an image. The scan size helps set the area of scanning. So a scan size of X equal to 12 micrometers means a scan area of 12 micrometers by 12 micrometers. The offset X, Y option allows

to specify X or Y scanner coordinates for the next scan to change the position of a scanned image. The scanner coordinates are the distance from the center of the scanner's range. The rotation option allows to change the scan direction from parallel to X axis to a certain degree angle to X axis. Scan rate is the speed at which scanning is done and for imaging in liquid a lower scan rate less than 0.5 Hz is normally chosen. The setpoint option allows the specification of the reference signal of the feedback loop. In Contact mode, setpoint is the value for the vertical force between the tip and the sample that results in bending of the cantilever. In Non-Contact mode, setpoint is the value for the amplitude of the cantilever's vibration. Tip bias allows to apply a bias voltage to the tip while sample bias enables to apply a bias voltage to the sample through magnetic sample holder. When non-contact mode AFM is selected there is an option to choose intermittent contact mode in the scan area control. In NC mode, drive is used for controlling the power of the drive amplitude needed for cantilever vibration. There is a unique called "scan here" which combines the approach and imaging functions and when the job is finished the tip is lifted automatically. The various features of the scan area control window is shown in fig A.3.

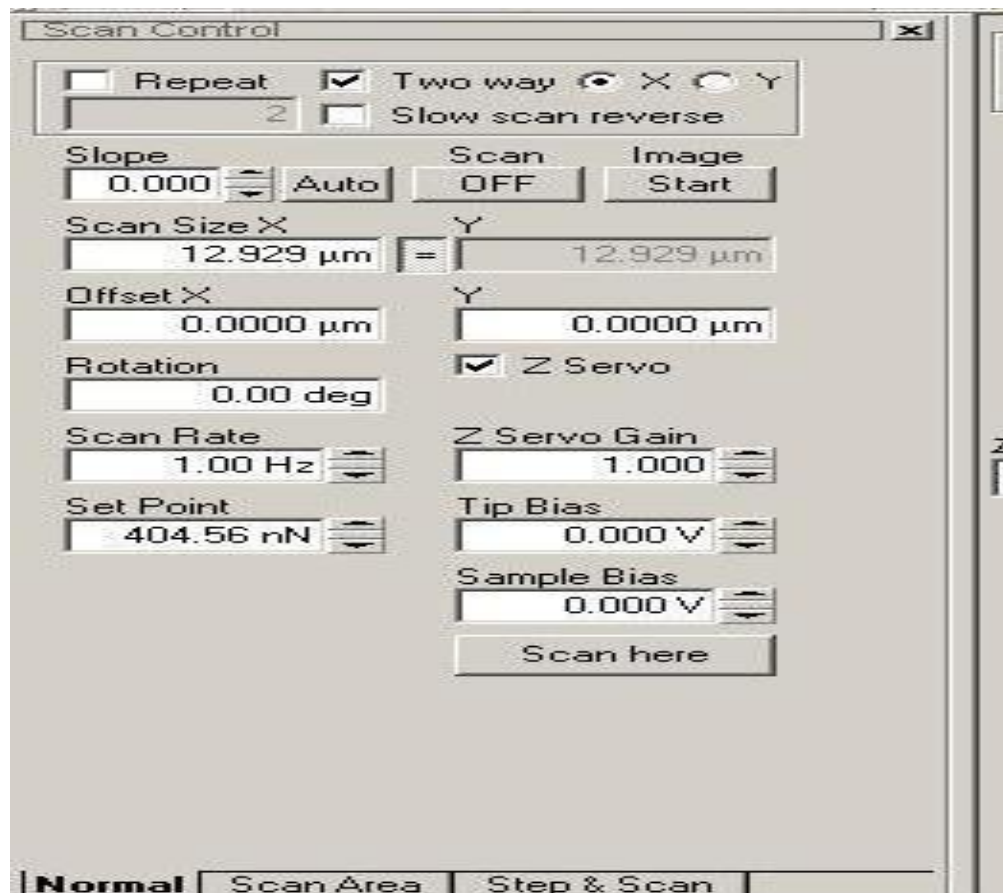


**Fig.A.3 A zoom to the scan control window**

There are two more modes in the scan area control window: scan area mode and step scan mode. In the Scan Area mode, the scan size can be varied as well as the X, Y offset by using a previously started image as a reference. At last, in Step & Scan mode, one can set the scan parameters at various positions for multiple imaging.

b) Trace control window: The window is basically an oscilloscope which is used to view signals in real time. Signals shown on the oscilloscope screen are obtained along the scanning direction. The signal obtained from the forward scan direction is shown by a yellow trace line on the Oscilloscope screen. If the backward scan direction is selected from the "Input Configuration window", a blue trace line will also be displayed on the screen. For good imaging, the blue and the yellow line should follow each other nicely in three windows: Amplitude, Phase and Topography. When this condition is met imaging can be started.

c) Monitor window : The Monitor window shows the quad-cell PSPD (Position Sensitive Photo Detector), having a cross-hair view with a black scale bar to its right, and three digital panels (A-B, C-D, A+B) in voltage units. In the same window, an Error signal bar is present and a Z scanner bar is there to view the status of the feedback loop and the Z scanner in real time while working with the XE system through XEP. In Custom tab, several input signals can be chosen and monitored through Digital panels in real time as shown in fig A.5.

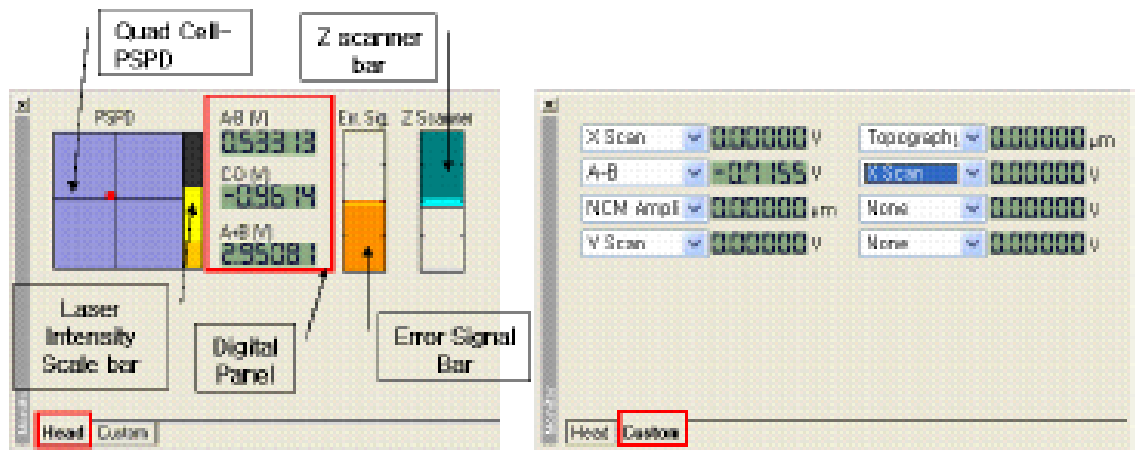


**Fig A.5: Labeled and zoomed view of the monitor window**

Quad cell PSPD shows the position of the reflected laser beam on the PSPD for monitoring the deflection of the cantilever. Laser Intensity scale bar gives a graphical view of the reflected laser beam generating a yellow bar proportional to it. A-B digital signal monitors the cantilever deflection and amplitude of cantilever vibration. A+B digital signal measures the intensity of reflected laser beam on quad cell PSPD. Error signal bar displays graphically the error signal value from PSPD relative to the set point value. Z scanner bar represents graphically the Z extension of the piezoelectric scanner within its total range.

d) Stage Control windows: The Z stage position and the focus stage values are shown in the Stage Control windows. They help to find the position to take an image and helps to

follow the position of the tip with the optical microscope, respectively. It's applied to two main stages of our interest: the motorized Z stage and the focus stage of the optical microscope as shown in Fig. A.6 below. The Lift Z button lifts the XE 100 head on to its default position at the start of the imaging cycle. The Approach button is normally used when the tip is within a 1 mm distance from the sample and it's risky to operate manually anymore. So, on being pressed the tip approaches automatically onto the sample surface.

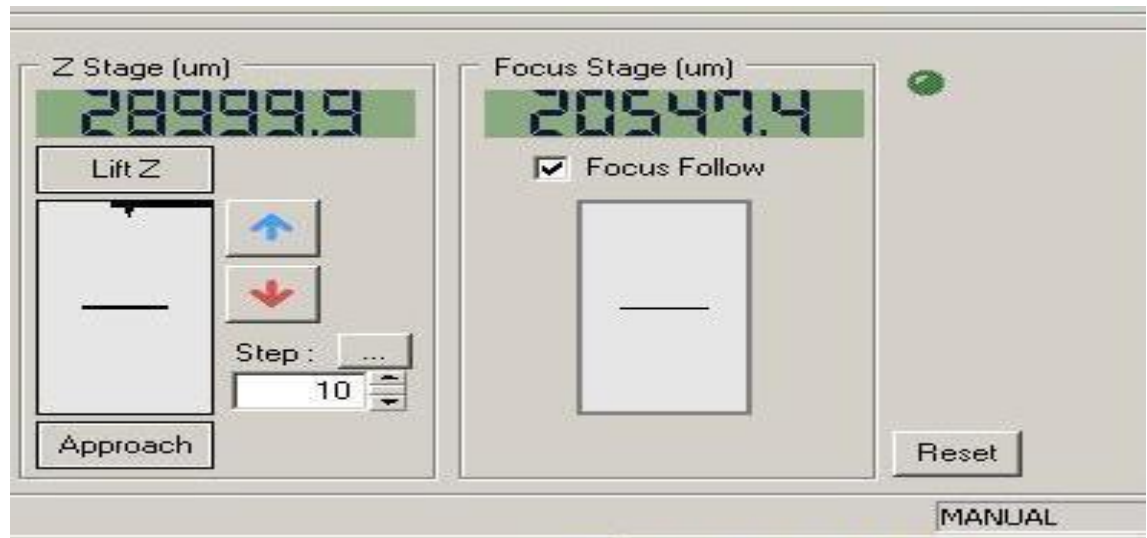


**Fig.A.6: A zoomed view of the Stage Control window.**

e) F/D Spectroscopy 2.0: A detailed description of the basics of Force distance Spectroscopy is provided in section 3.6 of this thesis. Here we keep our explanations limited to the understanding of force distance spectroscopy mode window found in the XEP software. The header bar of the XEP software has an option Mode which helps to select the mode in which to use the AFM. "Force Distance Spectroscopy 2.0" should be chosen. Fig.A.7 below presents a view of the Force distance Spectroscopy window as seen in the XEP software. Before proceeding to Force distance Spectroscopy it is very important to take an image of the sample in the scan mode. Even a half image or any partial image of the sample is alright as long as the user has a good idea of the topography of the sample and knows which portions of the sample to measure. The force distance spectroscopy interface window is divided into three important portions. One is the parameter window where the parameters for the force distance spectroscopy are set. The force distance spectroscopy curves as they are generated for each of the chosen points. The image window shows the image taken with the scan mode and on positioning the cursor and right clicking the option of adding points for force distance spectroscopy comes up. Another option which can be selected instead of "Add points" is the "Edit Map" Option in which the Image window is divided into 2x2 or 4X4 or even higher number of points depending upon the selection.

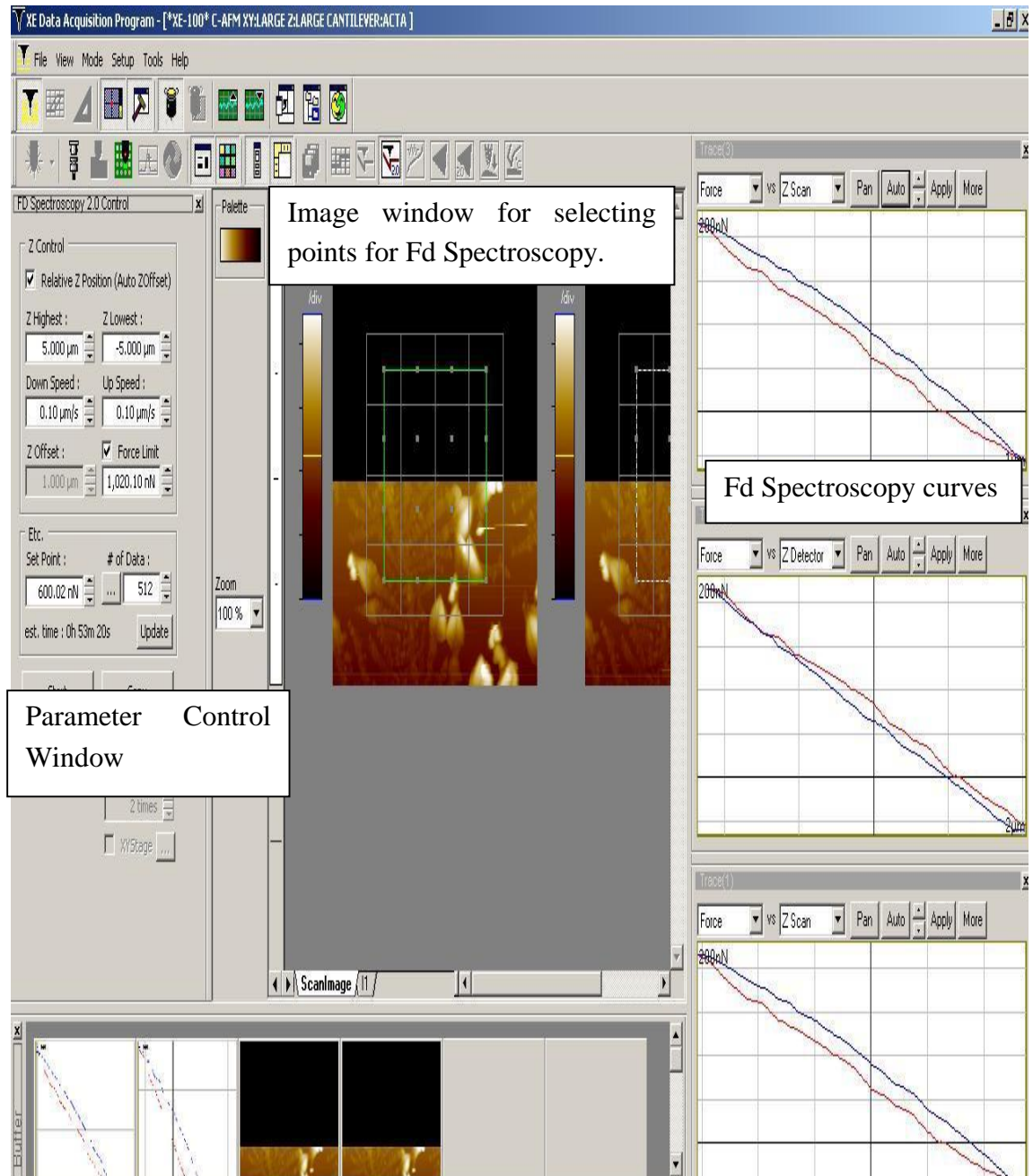


**Fig.A.7. XEP Force distance Spectroscopy 2.0 user interface.**

As already said, the parameters window shown above helps select the suitable parameters for the Force distance spectroscopy mode. A zoom of the Parameters control window is shown in Fig. A.8 below. There are five important parameters to control in the FD Spectroscopy 2.0 window.

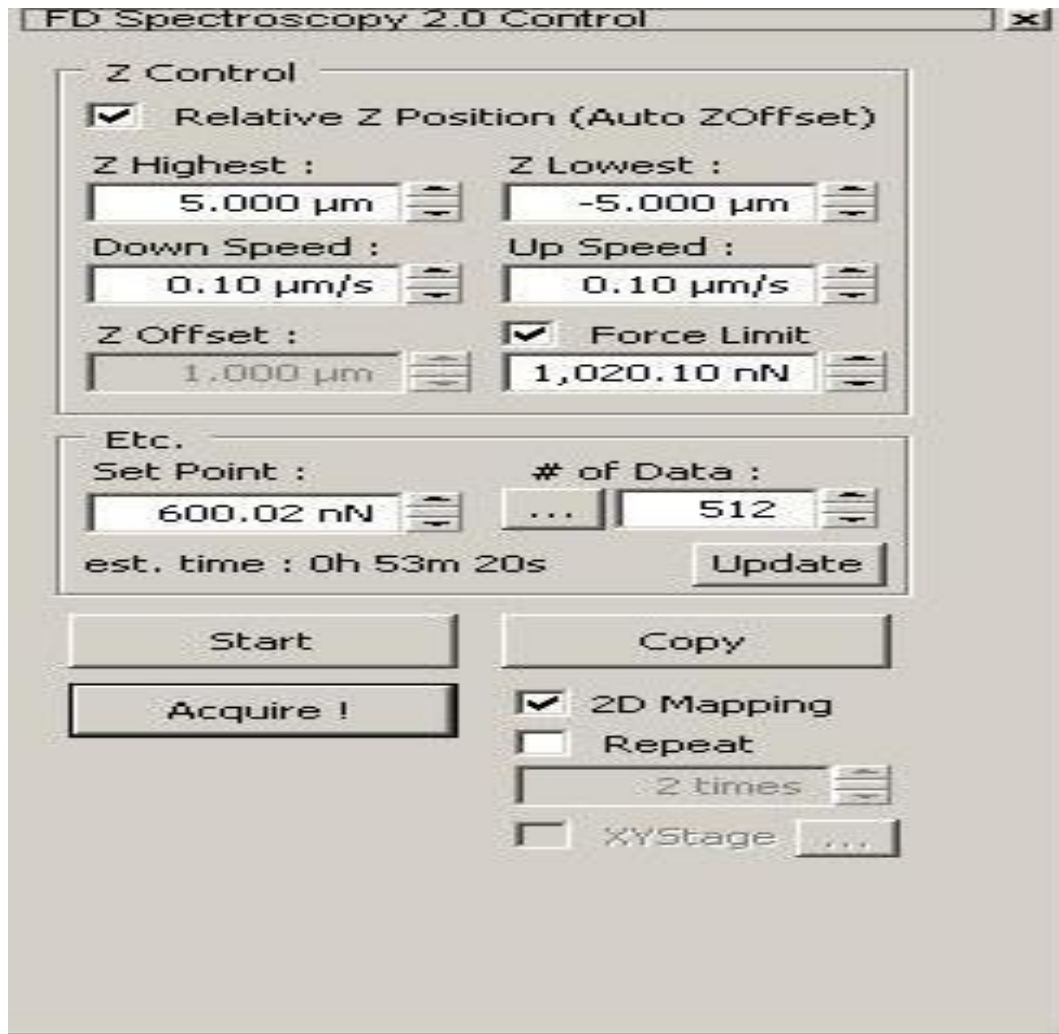


**Fig.A.8 Parameter Control window of the FD Spectroscopy 2.0.**

As seen above Z highest and Z lowest is used to limit the maximum distance the tip can penetrate into the sample. Down Speed and Up Speed is used to control the rate of approach of the tip towards and away from the sample respectively. The setpoint is used to range in which the force applied by the tip on the sample should be and it can be 40 to 70 per cent of the force limit. Force limit is the limiting or absolute value of the force exerted by the tip on the sample and if it exceeds beyond it then the cantilever might be damaged. Normally, each and every type of cantilever has its own Force limit and setpoint values depending on its specifications. As the specifications of the cantilever are fed in the XEP software part database, the FD Spectroscopy mode is able to calculate by itself the maximum value of the force limit. If the user tries to put a higher value than calculated by the software, it comes to the maximum force limit value calculated by the software.

### A.3 XEI Image Processing Software

The Park Systems XEI Image processing software is again a software with a huge number of features like the data processing software. However, here we keep our discussion limited to the most essential features of the software necessary for us. An overview of the software is presented in fig A.9 below.

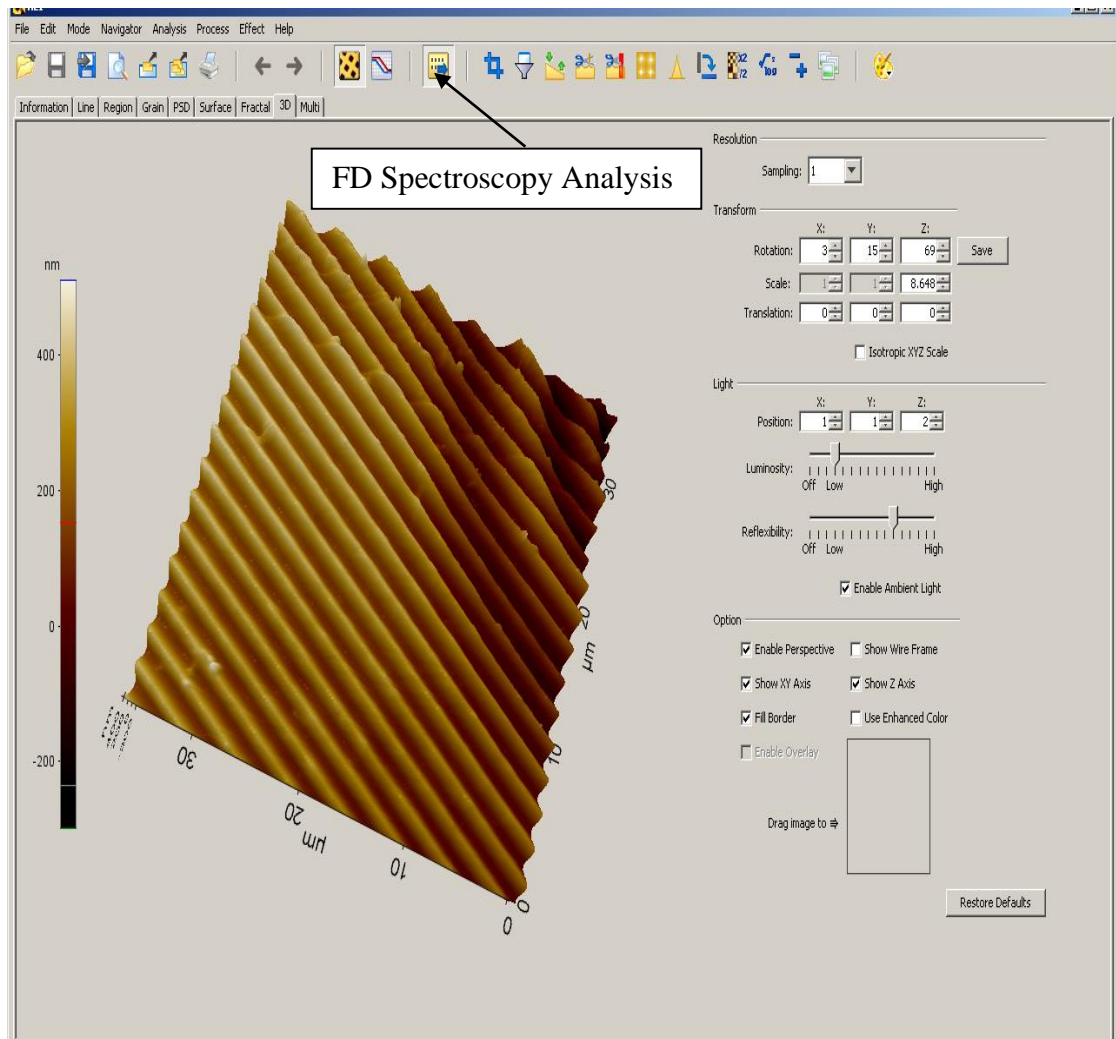


**Fig.A.9** An overview of the image processing section of the XEI software with the arrow showing the option for clicking F-d spectroscopy mode.

A 3 dimensional image of the topography can be seen here. The information section of the software gives a complete overview of the parameters used during imaging for example, information about the cantilever, date of imaging, mode of imaging, scan rate during imaging, Z Servo gain and area of the image. As it can be seen in Fig. 4.9, there is a separate button for selecting the force distance spectroscopy mode and that gives information on the force distance curves obtained at all the selected points in the topography of the image. Several such force distance curves were needed during the course of

the measurements to have an idea about the elasticity of samples as well as for measuring the beating force of cardiomyocytes. The Line selection in the software helps generate 2 dimensional lines of the topography of the image either in XZ axis or YZ axis as shown in Fig. A.10 .

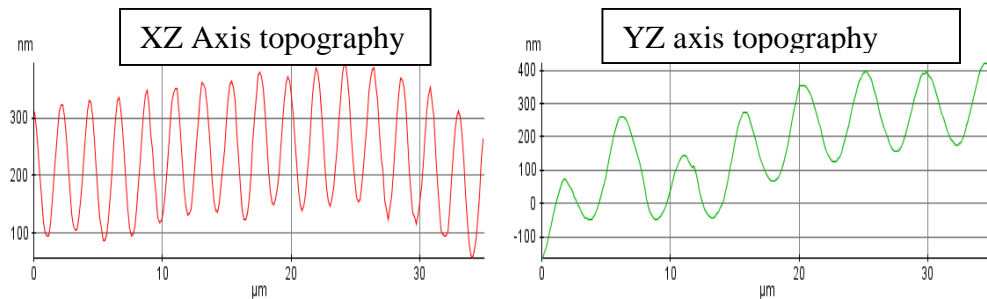


**Fig.A.10** Line profile of a sample 3D image with XEI software.

A click on the 3D button generates a 3 dimensional image of the sample topography and it's already shown in Fig. 4.9. There are several other useful features of this software but for the sake of brevity, I keep this discussion limited to the most important concepts.